Quantum-chromodynamic predictions for inclusive spin-spin asymmetries at large transverse momentum

John Babcock,* Evelyn Monsay, and Dennis Sivers
Argonne National Laboratory, High Energy Physics Division, Argonne, Illinois 60439
(Received 20 October 1978)

We discuss predictions for the asymmetry A_{LL} in the inclusive production at large p_T of charged and neutral pions by longitudinally polarized protons. We work in the framework of a hard-scattering model based on perturbative quantum chromodynamics. Various assumptions for the distribution of the proton's spin among its constituents—quarks, ocean antiquarks, and gluons—and the effects of scaling violations on the parton distributions are considered.

I. INTRODUCTION

The idea that the production of hadrons at large transverse momentum can be understood by a careful combination of the usual hard-scattering model with quantum-chromodynamics (QCD) perturbation theory has been gaining important support.[1] The first calculations of the fundamental $2 \to 2$ processes involving quarks and gluons to lowest order in perturbation theory[2,3] have recently been combined with a serious attempt to estimate the contribution of higher-order corrections in the form of nonscaling structure functions[4] and smearing in the quark-gluon transverse momenta.[1]

Since QCD is the only serious candidate currently available for a theory of the strong interactions, our capability of achieving quantitative fits to large-p_T production data from it is encouraging. However, it seems necessary to do experiments at very high energies ($\sqrt{s} \gtrsim 200$ GeV) to distinguish the QCD-based approach from other *ad hoc* models on the basis of single-particle inclusive measurements alone.[1] It is interesting, therefore, to explore other types of measurements which can be done with existing accelerators and which are sensitive to the fundamental hypothesis of Refs. 1–3—that the hard scattering which is responsible for large-p_T production is determined by QCD perturbation theory.

It is our contention that experiments using polarized beams and targets can play an important role in testing QCD. Quantum chromodynamics can be defined as the theory of spin-$\frac{1}{2}$ color-triplet quarks and spin-1 color-octet vector gluons interacting in a gauge-invariant manner. Spin plays an important dynamical role. In a previous paper[5] we pointed out the existence of distinctive spin-spin asymmetries (differences in the scattering cross section which depend on whether the helicities of the initial particles are aligned or not) in the fundamental $2 \to 2$ processes of QCD: $qq \to qq$, $q\bar{q} \to q\bar{q}$, $\bar{q}\bar{q} \to \bar{q}\bar{q}$, $qV \to qV$, $\bar{q}V \to \bar{q}V$, $q\bar{q} \to VV$, $VV \to q\bar{q}$, and $VV \to VV$. When combined with the reasonable assumption that quarks and gluons "remember" the spin of the protons containing them, these fundamental asymmetries give rise to an observable

$$A_{LL} = \frac{[d\sigma(p(+)p(+) \to \pi X) - d\sigma(p(+)p(-) \to \pi X)]}{[d\sigma(p(+)p(+) \to \pi X) + d\sigma(p(+)p(-) \to \pi X)]} \tag{1.1}$$

for inclusive production at large transverse momentum from a longitudinally polarized beam and target.

In this paper we would like to demonstrate how, in the context of the general hard-scattering model,[6] a spin-spin asymmetry in the fundamental 2-2 scattering processes can be responsible for an inclusive production asymmetry. We will also discuss some simple models for spin-dependent structure functions which we can use to make specific predictions for Eq. (1.1). Although at present not much is known about these functions (which determine how the spin of a proton is distributed among the fundamental quark and gluon constituents), measurements of spin asymmetries in electroproduction[7] and in the production of massive lepton pairs[8] can be used to determine the quark and antiquark distributions. When this has been done, the prediction of the QCD model for the large-p_T production asymmetry can be used to investigate the gluon spin distributions. The QCD-hard-scattering model can also be used to test the form of the fundamental quark-quark and quark-gluon interactions.

A measurement of the inclusive asymmetry A_{LL} involves many tough experimental questions. There currently exists the technical capability to build polarized proton beams using the parity-violating decay of Λ's produced at high-energy accelerators such as Fermilab and the CERN SPS,[9] and it therefore seems feasible that the type of experiment we discuss can be done within a few years.

It is important to note that the predictions for the

 ©1979 The American Physical Society

observable A_{LL} appear to be relatively insensitive to questions concerning scaling violations and k_T smearing in the quark and gluon distributions since both the cross sections involved in the ratio are affected in approximately the same way. Controversies regarding the proper way to implement these effects in QCD therefore do not necessarily invalidate our results.

The plan of the remainder of this paper is as follows: Section II presents a derivation of the expression for definite-helicity cross sections in the hard-scattering model. Section III gives the evaluation to lowest order in QCD perturbation theory of the fundamental spin-spin asymmetries. Section IV discusses some simple models for the spin-dependent distribution functions. In Sec. V we give the specific model calculations for the inclusive spin-spin observable for pp and for $\bar{p}p$ collisions. In Sec. VI we draw some conclusions concerning the interpretation of our results.

II. HARD-SCATTERING MODEL FOR DEFINITE-HELICITY CROSS SECTIONS

It is instructive to review the steps which enable us to predict an inclusive asymmetry such as given in Eq. (1.1). Our basic hypothesis is that we can combine the usual hard-scattering model[6] with perturbative QCD in the manner discussed in Refs. 1–3.

In the hard-scattering parton model, the interaction of two protons, A and B, is assumed to proceed through the scattering of the constituents a of proton A and b of proton B, with invariant cross section $(d\hat{\sigma}/d\hat{t})(ab \to cd)$. If we consider the spin-averaged case for the moment, the invariant cross section is given by

$$E\frac{d\sigma}{d^3p}(pp \to \pi X) = \sum_{ab\to cd}\int_{x_{a\,\min}}^{1} dx_a \int_{x_{b\,\min}}^{1} dx_b G_{a/A}(x_a) G_{b/B}(x_b) D_c^h(z_c) \frac{1}{z_c}\frac{1}{\pi}\frac{d\hat{\sigma}}{d\hat{t}}(ab \to cd), \tag{2.1}$$

where $G_{a/A}(x_a)$ is the probability of finding a parton of type a in proton A with fraction x_a of A's longitudinal momentum ($G_{b/B}$ is defined in a similar manner) and $D_c^h(z_c)$ is the probability that outgoing parton c decays into a hadron h with fraction z_c of the initial longitudinal momentum of the parton. We are assuming that these distributions scale (are functions of momentum fractions only), but the form is unchanged if higher-order corrections can be factorized and contributions absorbed into the distribution and decay functions at the cost of making these functions depend weakly on the momentum transfer. This factorization has been shown to be true to low orders in perturbation theory and is speculated to be true in general.[4]

The constituent scattering cross section $d\hat{\sigma}/d\hat{t}$ is a function of the parton center-of-mass variables

$$\begin{aligned}\hat{s} &= (p_a + p_b)^2 \cong x_a x_b s + \cdots,\\ \hat{t} &= (p_a - p_c)^2 \cong x_a t/z_c + \cdots,\\ \hat{u} &= (p_b - p_c)^2 \cong x_b u/z_c + \cdots,\end{aligned} \tag{2.2}$$

where we are neglecting (we hope small) transverse-momentum fluctuations of the constituents and where the usual Mandelstam variables are given by

$$\begin{aligned}s &= (p_A + p_B)^2,\\ t &= (p_A - p_h)^2,\\ u &= (p_B - p_h)^2,\end{aligned} \tag{2.3}$$

If we take the effective masses of the constituents to be zero, then $\hat{s}+\hat{t}+\hat{u} \cong 0$. Hence, the value of z_c is constrained, i.e.,

$$z_c \cong -\frac{t}{sx_b} - \frac{u}{sx_a}. \tag{2.4}$$

The lower limits of the x_a and x_b integrations in Eq. (2.1) are given by

$$\begin{aligned}x_{a_{\min}} &\cong x_\perp \cot(\theta/2)/[2 - x_\perp \tan(\theta/2)],\\ x_{b_{\min}} &\cong x_a x_\perp \tan(\theta/2)/[2x_a - x_\perp \cot(\theta/2)],\end{aligned} \tag{2.5}$$

where θ is the constituent c.m. scattering angle and $x_\perp = 2\sqrt{tu}/s = 2p_T/\sqrt{s}$ is the momentum of the detected hadron transverse to the direction of the incident protons divided by its maximum value.

When we consider the scattering of polarized protons, the distributions $G_{a/A}(x_a)$ and $G_{b/B}(x_b)$ must be generalized to allow for the transmission of spin information from the proton to its constituents. So, for the process $\vec{p}\vec{p} \to (\pi \text{ or jet}) + X$, as il-

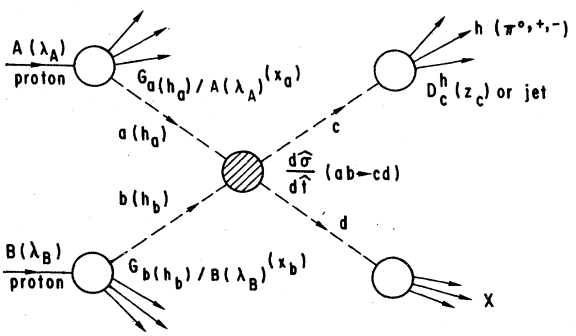

FIG. 1. Hard-scattering model for initially polarized protons.

lustrated in Fig. 1 we define distributions

$$G_{a(h_a)/A(\lambda_A)}(x_a),$$

the probability of finding a parton of type a and helicity h_a in proton A, of helicity λ_A, with fraction x_a of A's longitudinal momentum, and

$$G_{b(h_b)/B(\lambda_B)}(x_b),$$

which is defined in a similar manner. To find an expression for the invariant cross section,

$$E d\sigma_{\lambda_A\lambda_B}/d^3p,$$

analogous to Eq. (2.1) for the case of polarized proton scattering, let us represent the spin-dependent part of the integrand of $E d\sigma_{\lambda_A\lambda_B}/d^3p$ by

$$d\sigma_{A(\lambda_A)B(\lambda_B)}$$

and let $(d\hat{\sigma}/d\hat{t})h_a h_b$ denote the c.m. cross section for constituents a and b having positive ($h_{a,b}=+$) or negative ($h_{a,b}=-$) helicity. Then we can write schematically

$$d\sigma_{A(+)B(+)} = G_{a(+)/A(+)}G_{b(+)/B(+)}\frac{d\hat{\sigma}_{++}}{d\hat{t}} + G_{a(+)/A(+)}G_{b(-)/B(+)}\frac{d\hat{\sigma}_{+-}}{d\hat{t}} + G_{a(-)/A(+)}G_{b(+)/B(+)}\frac{d\hat{\sigma}_{-+}}{d\hat{t}} + G_{a(-)/A(+)}G_{b(-)/B(+)}\frac{d\hat{\sigma}_{--}}{d\hat{t}}, \tag{2.6}$$

$$d\sigma_{A(+)B(-)} = G_{a(+)/A(+)}G_{b(+)/B(-)}\frac{d\hat{\sigma}_{++}}{d\hat{t}} + G_{a(+)/A(+)}G_{b(-)/B(-)}\frac{d\hat{\sigma}_{+-}}{d\hat{t}} + G_{a(-)/A(+)}G_{b(+)/B(-)}\frac{d\hat{\sigma}_{-+}}{d\hat{t}} + G_{a(-)/A(+)}G_{b(-)/B(-)}\frac{d\hat{\sigma}_{--}}{d\hat{t}}. \tag{2.7}$$

We are suppressing the integration and kinematic variables which are the same as in the spin-averaged case. It is convenient to deal with the sums and differences of the distribution functions and constituent cross sections. We define

$$\begin{aligned}
\Delta G_{a/A} &= (G_{a(+)/A(+)} - G_{a(-)/A(+)}),\\
\Delta G_{b/B} &= (G_{b(+)/B(+)} - G_{b(-)/B(+)}),\\
\frac{\Delta d\hat{\sigma}}{d\hat{t}} &= \frac{d\hat{\sigma}_{++}}{d\hat{t}} - \frac{d\hat{\sigma}_{+-}}{d\hat{t}},
\end{aligned} \tag{2.8}$$

and also note that the distributions and constituent cross sections entering into Eq. (2.1) are given by

$$\begin{aligned}
G_{a/A} &= G_{a(+)/A(+)} + G_{a(-)/A(+)},\\
G_{b/B} &= G_{b(+)/B(+)} + G_{b(-)/B(+)},\\
\frac{d\hat{\sigma}}{d\hat{t}} &= \frac{1}{2}\left(\frac{d\hat{\sigma}_{++}}{d\hat{t}} + \frac{d\hat{\sigma}_{+-}}{d\hat{t}}\right).
\end{aligned} \tag{2.9}$$

The parity invariance of the strong interaction implies that

$$\begin{aligned}
G_{b(+)/B(-)} &= G_{b(-)/B(+)},\\
G_{b(-)/B(-)} &= G_{b(+)/B(+)},\\
\frac{d\hat{\sigma}_{++}}{d\hat{t}} &= \frac{d\hat{\sigma}_{--}}{d\hat{t}}, \quad \frac{d\hat{\sigma}_{+-}}{d\hat{t}} = \frac{d\hat{\sigma}_{-+}}{d\hat{t}}.
\end{aligned} \tag{2.10}$$

By using the definitions of Eq. (2.8) and the results of parity invariance given in Eq. (2.10), we can write

$$\begin{aligned}
d\sigma_{A(+)B(+)} - d\sigma_{A(+)B(-)} &= \left(\frac{d\hat{\sigma}_{++}}{d\hat{t}} - \frac{d\hat{\sigma}_{+-}}{d\hat{t}}\right)(G_{a(+)/A(+)}G_{b(+)/B(+)} - G_{a(+)/A(+)}G_{b(-)/B(+)}\\
&\quad - G_{a(-)/A(+)}G_{b(+)/B(+)} + G_{a(-)/A(+)}G_{b(-)/B(+)})\\
&= \left(\Delta\frac{d\hat{\sigma}}{d\hat{t}}\right)(\Delta G_{a/A})(\Delta G_{b/B}).
\end{aligned} \tag{2.11}$$

Hence, we find that the expression for the difference of invariant cross sections for the process $\vec{p}\vec{p} \to \pi X$ can be written as

$$\left(\frac{E d\sigma_{++}}{d^3p} - \frac{E d\sigma_{+-}}{d^3p}\right) \cong \sum_{ab\to cd}\int_{x_a\,\min}^{1} dx_a \int_{x_b\,\min}^{1} dx_b \left[\Delta G_{a/A}(x_a)\Delta G_{b/B}(x_b) D_c^{\pi}(z_c)\frac{1}{\pi}\,\frac{1}{z_c}\left(\frac{\Delta d\hat{\sigma}}{d\hat{t}}\right)\right], \tag{2.12}$$

where z_c is given by Eq. (2.4). Now, in terms of the invariant cross sections given in Eqs. (2.1) and (2.12), we can write the asymmetry A_{LL} defined in Eq. (1.1) as

$$A_{LL}=\frac{\left(\frac{Ed\sigma_{++}}{d^3p}-\frac{Ed\sigma_{+-}}{d^3p}\right)}{\frac{2Ed\sigma}{d^3p}}. \tag{2.13}$$

It should be noted that the fundamental assumption of the hard-scattering model that justifies the incoherent formula (2.1) implies that single-spin asymmetries (or polarizations) should vanish. This assumption can no longer be strictly correct in the presence of scaling violations associated with coherent processes. The experimental measurement of inclusive one-spin asymmetries provides a possible test for the effect of coherent dynamics on the generalized hard-scattering model. The existence of nontrivial A dependence in scattering off nuclear targets is a clue that they are present.[10] Much more theoretical work is involved in the prediction of polarization than in the spin-spin asymmetries discussed here, but we cannot ignore their interrelation. Measurement of a sizable ($\gtrsim 30\%$) single-spin asymmetry would call into question the assumptions under which the predictions of the two spin asymmetries are made. Because spin observables are interrelated, there would be feedback from polarization on spin-spin asymmetries.

In order to evaluate the expression for A_{LL} of Eq. (2.13), we must determine the constituent cross sections and the distributions of Eq. (2.8). We now turn to the problem of obtaining them.

III. EVALUATION OF QCD CROSS SECTIONS FOR DEFINITE-HELICITY QUARKS AND GLUONS

We would like to give here the expressions for the differential cross sections for the scattering of quarks and gluons from states of definite helicity. The cross sections are calculated to lowest order in the perturbation expansion for QCD. We neglect terms involving the mass of the quarks. The assumptions involved in using these cross sections in the hard-scattering model are discussed in Refs. 1–3. We include some of the details involved in the calculation in order that the reader may judge to what extent the spin degrees of freedom for the quarks and gluons are playing a fundamental role in the dynamics.

A. The process $q_\alpha q_\beta \to q_\alpha q_\beta$

The diagrams for $qq \to qq$ are

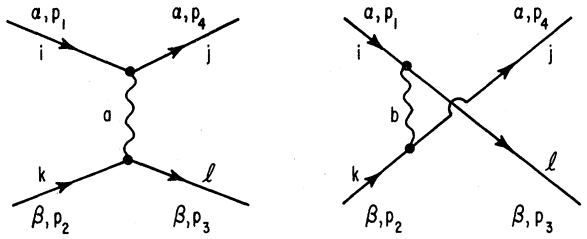

(t channel) (u channel)

$i, j, k, l = 1\text{–}3$ (quark color),

$a, b = 1\text{–}8$ (gluon color),

$\alpha, \beta = u, d\ldots$ (quark flavor),

$s=(p_1+p_2)^2$, $t=(p_1-p_4)^2$, $u=(p_1-p_3)^2$.

In the Feynman gauge the amplitudes can be written in the form

$$\begin{aligned}\mathfrak{M}_t &= \frac{g^2}{t}(T^a_{ij}T^a_{kl})\bar{u}^j_\alpha(p_4,h_4)\gamma_\mu u^i_\alpha(p_1,h_1)\\ &\quad\times \bar{u}^l_\beta(p_3,h_3)\gamma^\mu u^k_\beta(p_2,h_2),\\ \mathfrak{M}_u &= \frac{-g^2}{u}(T^b_{il}T^b_{kj})\delta_{\alpha\beta}\bar{u}^j_\alpha(p_4,h_4)\gamma_\nu u^k_\beta(p_2,h_2)\\ &\quad\times \bar{u}^l_\beta(p_3,h_3)\gamma^\nu u^i_\alpha(p_1,h_1).\end{aligned} \tag{3.1}$$

The $\delta_{\alpha\beta}$ indicates that the u-channel term is present only when the quarks are identical. We then use the projection operators for definite helicity appropriate for zero-mass quarks

$$\begin{aligned}&u(p,h)\bar{u}(p,h)=\tfrac{1}{2}(1+h\gamma_5)\not{p},\\ &v(p,h)\bar{v}(p,h)=\tfrac{1}{2}(1-h\gamma_5)\not{p},\\ &\sum_{\text{spins}} u(p,h)\bar{u}(p,h)=\sum_{\text{spins}} v(p,h)\bar{v}(p,h)=\not{p}.\end{aligned} \tag{3.2}$$

The color matrices are defined $T^a_{ij}=\frac{1}{2}\lambda^a_{ij}$ where the λ^a are the usual Gell-Mann matrices for SU(3). The color traces are given in Ref. 2. Averaging over initial colors and summing over final colors and spins, we find

$$\begin{aligned}&|\mathfrak{M}|^2_{h_1h_2}=(\tfrac{1}{9})\sum_{\text{color}}\sum_{\substack{\text{final}\\ \text{spin}}}|\mathfrak{M}_{t_{h_1h_2}}+\mathfrak{M}_{u_{h_1h_2}}|^2,\\ &|\mathfrak{M}|^2_{++}=(\tfrac{8}{9})g^4\left[\frac{s^2}{t^2}+\delta_{\alpha\beta}\left(\frac{s^2}{u^2}-\frac{2}{3}\frac{s^2}{tu}\right)\right],\\ &|\mathfrak{M}|^2_{+-}=(\tfrac{8}{9})g^4\left(\frac{u^2}{t^2}+\delta_{\alpha\beta}\frac{t^2}{u^2}\right).\end{aligned} \tag{3.3}$$

Parity invariance guarantees

$$|\mathfrak{M}|^2_{--}=|\mathfrak{M}|^2_{++},\quad |\mathfrak{M}|^2_{-+}=|\mathfrak{M}|^2_{+-}. \tag{3.4}$$

For nonidentical quarks, the fact that $|\mathfrak{M}|^2_{+-}$

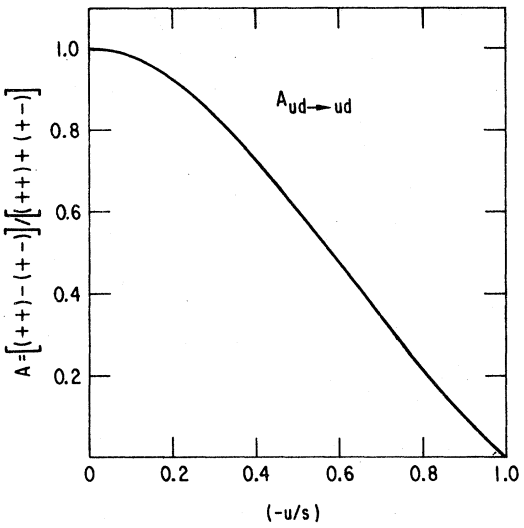

FIG. 2. Constituent asymmetry for unlike-flavored quarks as a function of $(-u/s)$.

vanishes in the backward direction ($u=0$) can be obtained by combining the helicity conservation of the γ_μ vertex with the constraint of angular momentum conservation. The asymmetry

$$A=(|\mathfrak{M}|^2_{++}-|\mathfrak{M}|^2_{+-})/(|\mathfrak{M}|^2_{++}+|\mathfrak{M}|^2_{+-}) \qquad (3.5)$$

for unlike quarks (e.g. $ud\to ud$) is plotted against $(-u/s)$ in Fig. 2. For identical flavors, the asymmetry (3.5) is plotted in Fig. 3.

Using C invariance, the expressions (3.3) for $qq\to qq$ can also be used for $\bar{q}\bar{q}\to\bar{q}\bar{q}$.

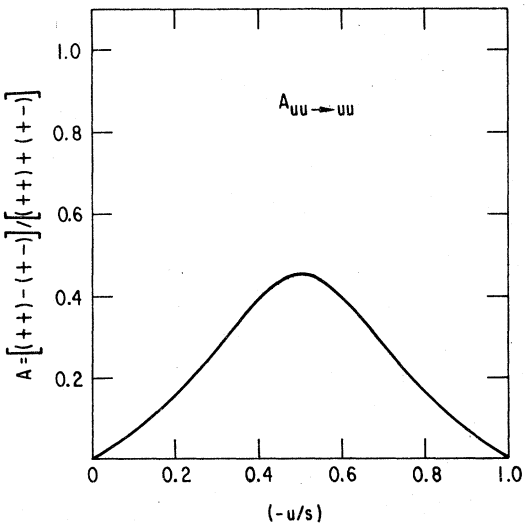

FIG. 3. Constituent asymmetry for like-flavored quarks as a function of $(-u/s)$.

B. The process $q_\alpha\bar{q}_\beta\to q_\delta\bar{q}_\gamma$

We can cross our diagrams for $qq\to qq$ to get those for $q\bar{q}\to q\bar{q}$ except that we now have to be more careful of the possibilities for different flavor combinations. The diagrams are

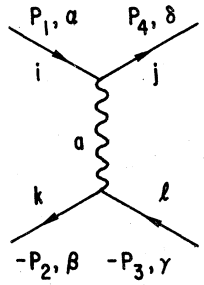

(t channel)

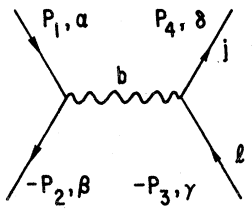

(s channel)

$i,j,k,l=1$–3 (quark color),

$a,b=1$–8 (gluon color),

$\alpha,\beta,\delta,\gamma=u,d,\ldots$ (quark flavor),

$s=(p_1+p_2)^2$, $t=(p_1-p_4)^2$, $u=(p_1-p_3)^2$.

The t-channel and s-channel amplitudes are

$$\mathfrak{M}_t(q_\alpha\bar{q}_\beta\to q_\delta\bar{q}_\gamma)=\frac{g^2}{t}\,\delta_{\alpha\delta}\delta_{\beta\gamma}T^a_{ij}T^a_{ik}\times\bar{u}^i_\delta(p_4,h_4)\gamma_\mu u^i_\alpha(p_1,h_1)\times\bar{v}^k_\beta(p_2,h_2)\gamma^\mu v^l_\gamma(p_3,h_3), \qquad (3.6)$$

$$\mathfrak{M}_s(q_\alpha\bar{q}_\beta\to q_\delta\bar{q}_\gamma)=\frac{-g^2}{s}\,\delta_{\alpha\beta}\delta_{\delta\gamma}T^b_{ik}T^b_{lj}\times\bar{u}^l_\delta(p_4,h_4)\gamma_\nu v^l_\gamma(p_3,h_3)\times\bar{v}^k_\beta(p_2,h_2)\gamma^\nu u^i_\alpha(p_1,h_1).$$

Using standard trace techniques we get

$$|\mathfrak{M}|^2_{++}=(\tfrac{8}{9})g^4\left(\delta_{\alpha\delta}\delta_{\beta\gamma}\,\frac{s^2}{t^2}\right),$$

$$|\mathfrak{M}|^2_{+-}=(\tfrac{8}{9})g^4\left[\delta_{\alpha\delta}\delta_{\beta\gamma}\,\frac{u^2}{t^2}+\delta_{\alpha\beta}\delta_{\delta\gamma}\,\frac{(t^2+u^2)}{s^2}-\tfrac{2}{3}\delta_{\alpha\delta}\delta_{\alpha\beta}\delta_{\delta\gamma}\,\frac{u^2}{st}\right]. \qquad (3.7)$$

For unlike flavors ($u\bar{d}\to u\bar{d}$) the asymmetry is the same as for $ud\to ud$ in Fig. 2. For flavor annihilation the asymmetry is -1 everywhere—a familiar result which is identical to that for $e^+e^-\to\mu^+\mu^-$. For $u\bar{u}\to u\bar{u}$ the asymmetry (3.5) is shown in Fig. 4.

C. The process $qV \to qV$

The diagrams for $qV \to qV$ are

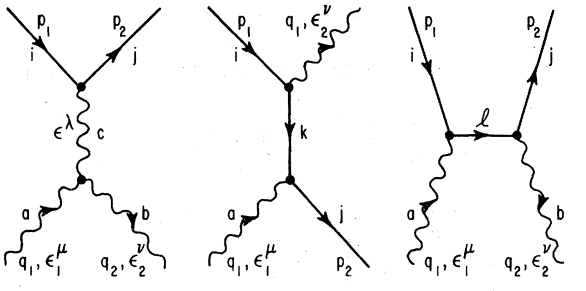

(t channel) (u channel) (s channel)

$i, j, k, l = 1$–3 (quark color),

$a, b, c = 1$–8 (gluon color),

$\mu, \nu, \lambda =$ Lorentz indices,

$s = (p_1 + q_1)^2$, $t = (p_1 - p_2)^2$, $u = (p_1 - q_2)^2$.

Defining a Lorentz tensor which occurs in the three-gluon vertex,

$$C^{\mu\lambda\nu}(q_1, q_2, q_3) \equiv [(q_1 - q_2)^\nu g^{\mu\lambda} + (q_2 - q_3)^\mu g^{\lambda\nu} + (q_3 - q_1)^\lambda g^{\mu\nu}], \tag{3.8}$$

we suppress the flavor indices and write the invariant amplitude from the three graphs shown above in the form

$$\mathfrak{M}(q_i V_a \to q_j V_b) = -g^2 \bar{u}_j(p_2, h_2)\left[\frac{if^{cab}}{t} T^c_{ij} \epsilon_1^\mu \epsilon_2^\nu \gamma^\lambda C_{\lambda\mu\nu}(q_1 - q_2, -q_1, q_2) + \frac{T^b_{ik} T^a_{kl}}{u} \not{\epsilon}_1(\not{p}_1 - \not{q}_2)\not{\epsilon}_2 + \frac{T^a_{il} T^b_{lj}}{s} \not{\epsilon}_2(\not{p}_1 + \not{q}_1)\not{\epsilon}_1\right] u_i(p_1, h_1). \tag{3.9}$$

In addition to the projection operators for definite-helicity quarks given by Eq. (3.2) we also need to use projection operators for definite-helicity gluons. We choose to project out the helicity for a gluon with momentum q,

$$\epsilon^\mu(q, \lambda)\epsilon^{*\nu}(q, \lambda) = \frac{1}{2}\left(-g^{\mu\nu} + \frac{q^\mu p^\nu + p^\nu q^\mu}{p \cdot q} - \frac{i\lambda\epsilon^{\mu\nu\alpha\beta} q^\alpha p^\beta}{p \cdot q}\right), \tag{3.10}$$

where $p^2 = 0$. Averaging over initial colors and summing over final spins and colors gives

$$|\mathfrak{M}|^2_{++} = g^4\left(\frac{2s^2}{t^2} - \frac{8}{9}\frac{s^2}{us}\right),$$
$$|\mathfrak{M}|^2_{+-} = g^4\left(\frac{2u^2}{t^2} - \frac{8}{9}\frac{u^2}{us}\right). \tag{3.11}$$

Again, angular momentum conservation and helicity conservation for the quark force $|\mathfrak{M}|^2_{+-}$ to vanish in the backward direction. The asymmetry given by Eq. (3.11) is plotted in Fig. 5.

The expressions for the cross sections for $\bar{q}V \to \bar{q}V$ are the same as those for $qV \to qV$.

D. The process $VV \to q\bar{q}$

The diagrams for $VV \to q\bar{q}$ are related to those for $qV \to qV$ by crossing. The diagrams are

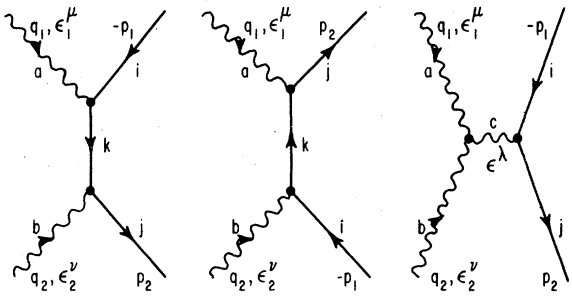

(t channel) (u channel) (s channel)

We can write the invariant amplitude

$$\mathfrak{M}(V_a(\lambda_a)V_b(\lambda_b) \to \bar{q}_i q_j) = -g^2 \bar{u}_j(p_2)\left[T^a_{ik} T^b_{kj} \not{\epsilon}_2(q_2, \lambda_b) \frac{(\not{q}_1 - \not{p}_1)}{t} \not{\epsilon}_1(q_1, \lambda_a) + T^b_{ik} T^a_{kj} \not{\epsilon}_1(q_1, \lambda_a) \frac{(\not{q}_2 - \not{p}_1)}{u} \not{\epsilon}_2(q_2, \lambda_b) + if^{abc} T^c_{ij} \frac{\epsilon_1^\mu(q_1, \lambda_a)\epsilon_2^\nu(q_2, \lambda_b)\gamma^\lambda}{s} C_{\mu\nu\lambda}(-q_1, -q_2, q_1 + q_2)\right] v_i(p_1). \tag{3.12}$$

Using Eq. (3.10) to project our definite-helicity gluons we get

$$|\mathfrak{M}^2|_{++} = 0,$$
$$|\mathfrak{M}^2|_{+-} = \left(\frac{1}{3}\frac{u^2 + t^2}{ut} - \frac{3}{4}\frac{u^2 + t^2}{s^2}\right). \tag{3.13}$$

E. The process $q\bar{q} \to VV$

The diagrams for $VV \to q\bar{q}$ are also appropriate for $q\bar{q} \to VV$ after changing the signs of the momenta. Although we now sum over gluon spins and project out specific quark spins, the answers

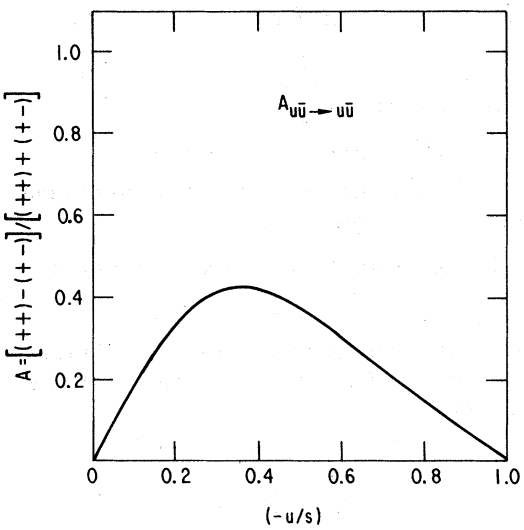

FIG. 4. Constituent asymmetry for quark-antiquark scattering like-flavored quarks as a function of $(-u/s)$.

$$|\mathfrak{M}^2|_{++}=0,$$
$$|\mathfrak{M}^2|_{+-}=\left(\frac{64}{27}\frac{t^2+u^2}{ut}-\frac{16}{3}\frac{t^2+u^2}{s^2}\right) \tag{3.14}$$

differ only by color-averaging factors from Eq. (3.13).

F. The process $VV\to VV$

The diagrams for gluon-gluon scattering are

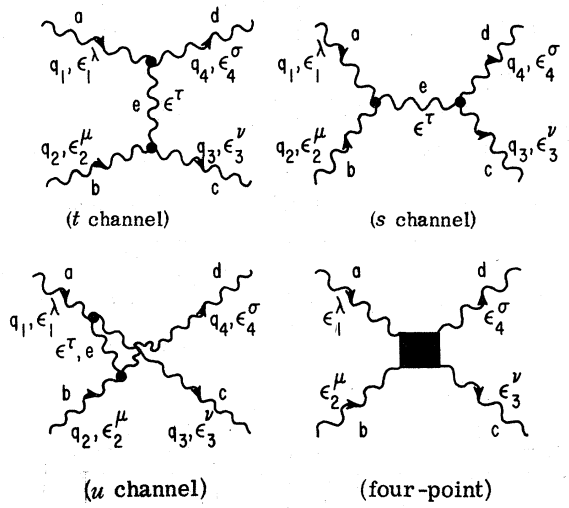

We can write the invariant amplitude in the form

$$\begin{aligned}\mathfrak{M}=-g^2\epsilon_1^\lambda(q_1,\lambda_1)\epsilon_2^\mu(q_2,\lambda_2)\epsilon_3^\nu(q_3)\epsilon_4^\sigma(q_4)\Big[&f_{aed}f_{ebc}C^{\lambda\tau\sigma}(-q_1,q_1-q_4,q_4)\frac{g_{\tau\tau'}}{t}C^{\tau'\mu\nu}(q_2-q_3,-q_2,q_3)\\&+f_{aec}f_{ebd}C^{\lambda\tau\nu}(-q_1,q_1-q_3,q_3)\frac{g_{\tau\tau'}}{u}C^{\tau'\mu\sigma}(q_2-q_4,-q_2,q_4)\\&+f_{abe}f_{cde}C^{\lambda\mu\tau}(-q_1,-q_2,q_1+q_2)\frac{g_{\tau\tau'}}{s}C^{\tau'\nu\sigma}(-q_3-q_4,q_3,q_4)\\&+f_{abe}f_{cde}(g^{\lambda\nu}g^{\mu\sigma}-g^{\lambda\sigma}g^{\mu\nu})+f_{ace}f_{bde}(g^{\lambda\mu}g^{\nu\sigma}-g^{\lambda\sigma}g^{\mu\nu})\\&+f_{ade}f_{cbe}(g^{\lambda\nu}g^{\mu\sigma}-g^{\lambda\mu}g^{\sigma\nu})\Big].\end{aligned} \tag{3.15}$$

Using Eq. (3.10) to project our initial spins, summing over initial colors and averaging over final colors and spins gives

$$|\mathfrak{M}^2|_{++}=\left(\frac{9}{2}\right)\left(\frac{2s^2}{ut}-\frac{su}{t^2}-\frac{st}{u^2}\right),$$
$$|\mathfrak{M}^2|_{+-}=\left(\frac{9}{2}\right)\left(6-\frac{2s^2}{ut}-\frac{su}{t^2}-\frac{st}{u^2}-\frac{2ut}{s^2}\right). \tag{3.16}$$

The asymmetry implied by these expressions is shown in Fig. 6.

Insofar as the sign and shape of the constituent asymmetries represent fundamental constraints such as approximate helicity conservation for light quarks and angular momentum conservation, they are not likely to be substantially changed by higher-order corrections.

A summary of the cross sections evaluated in this section is given in Table I.

IV. DISTRIBUTION FUNCTIONS FOR QUARKS AND GLUONS IN A SPINNNING PROTON

A. General discussion

Our ability to calculate a spin-spin asymmetry in large-p_T hadron production depends on the assumption that the spins of the fundamental constituents involved in the hard scattering are influenced by the spins of the external hadrons. In the quark-parton model, this influence is parametrized in terms of the distribution functions $G_{a(+)/A(+)}(x)$, $G_{a(-)/A(+)}(x)$, and $\Delta G_{a/A}(x)$ defined in Sec. II. It is

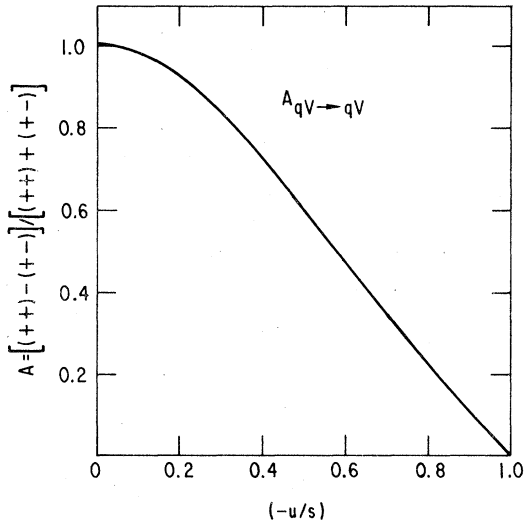

FIG. 5. Constituent asymmetry for quark-gluon scattering as a function of $(-u/s)$.

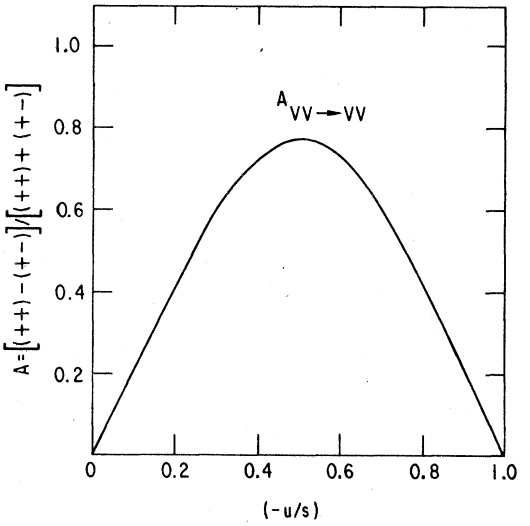

FIG. 6. Constituent asymmetry for gluon-gluon scattering as a function of $(-u/s)$.

now known that in QCD calculations we can reproduce the effect of certain higher-order perturbative corrections by allowing the distribution functions to have a mild dependence on the momentum transfer.[4] The form of this Q^2 dependence, or scaling violation, is considered to be a test of the underlying theory. For simplicity of notation in what follows we will usually omit displaying explicitly the Q^2 dependence of the structure functions in formulas. We will, as a first approximation, consider the functions to be independent of Q^2. Later we will return to the question of scaling violations and will use the formalism of Altarelli and Parisi[11] to examine corrections to this assumption.

In polarized eN or μN scattering experiments we can determine the structure functions[12]

TABLE I. Table of QCD cross sections for definite-helicity states. All cross sections contain a common factor $\pi\alpha_s^2/s^2$.

Process $ab\to cd$	$d\sigma/dt(a(+)b(+)\to cd)$	$d\sigma/dt(a(+)b(-)\to cd)$
$q_\alpha q_\beta \to q_\alpha q_\beta$	$\frac{8}{9}\left[\frac{s^2}{t^2}+\delta_{\alpha\beta}\left(\frac{s^2}{u^2}-\frac{2}{3}\right)\frac{s^2}{tu}\right]$	$\frac{8}{9}\left(\frac{u^2}{t^2}+\delta_{\alpha\beta}\frac{t^2}{u^2}\right)$
$q_\alpha \bar{q}_\beta \to q_\delta \bar{q}_\gamma$	$\frac{8}{9}\left(\delta_{\alpha\beta}\delta_{\beta\gamma}\frac{s^2}{t^2}\right)$	$\frac{8}{9}\left[\delta_{\alpha\delta}\delta_{\beta\gamma}\frac{u^2}{t^2}+\delta_{\alpha\beta}\delta_{\delta\gamma}\frac{(t^2+u^2)}{s^2}-\frac{2}{3}\delta_{\alpha\gamma}\delta_{\alpha\beta}\delta_{\delta\gamma}\frac{u^2}{st}\right]$
$qV \to qV$	$\left(\frac{2s^2}{t^2}-\frac{8}{9}\frac{s^2}{us}\right)$	$\left(\frac{2u^2}{t^2}-\frac{8}{9}\frac{u^2}{us}\right)$
$\bar{q}V \to \bar{q}V$	$\left(\frac{2s^2}{t^2}-\frac{8}{9}\frac{s^2}{us}\right)$	$\left(\frac{2u^2}{t^2}-\frac{8}{9}\frac{u^2}{us}\right)$
$VV \to q\bar{q}$	0	$\left[\frac{1}{3}\frac{(u^2+t^2)}{ut}-\frac{3}{4}\frac{(t^2+u^2)}{s^2}\right]$
$q\bar{q} \to VV$	0	$\left(\frac{64}{27}\frac{t^2+u^2}{ut}-\frac{16}{3}\frac{t^2+u^2}{s^2}\right)$
$VV \to VV$	$\frac{9}{2}\left(\frac{2s^2}{ut}-\frac{su}{t^2}-\frac{st}{u^2}\right)$	$\frac{9}{2}\left(6-\frac{2s^2}{ut}-\frac{su}{t^2}-\frac{st}{u^2}-\frac{2ut}{s^2}\right)$

$$f^N(x)=\sum_q (e_q)^2[G_{q/N}(x)+G_{\bar{q}/N}(x)] \tag{4.1}$$

and

$$g_1^N(x)=\frac{1}{2}\sum_q (e_q)^2[\Delta G_{q/N}(x)+\Delta G_{\bar{q}/N}(x)]\,, \tag{4.2}$$

where $x=Q^2/2m\nu$ is the usual Bjorken scaling variable and it is assumed we are in the deep-inelastic regime. We are interested here in helicities, so a third structure function, conventionally labeled $g_2^N(x)$, which involves spins in a transversity basis, does not enter into our expressions. Note that good data on polarized leptoproduction can be used to obtain directly the distributions $\Delta G_{q/p}(x)$ and $\Delta G_{\bar{q}/p}(x)$ for quarks and antiquarks but that the gluon asymmetries cannot be measured in this way. At this time, measurements of the polarized leptoproduction asymmetry have not been carried out at all values of x.[13,14] In order to display definite calculations we therefore resort to some simple theoretical models in order to obtain distributions.

For convenience we will define $u(x)$, $d(x)$, $\bar{u}(x)$, etc. to be the distribution functions for up, down, antiup, etc. quarks in the proton as given, for example, by Feynman.[12] The differences $G_{u(+)/p(+)}(x)-G_{u(-)/p(+)}(x)$ will be denoted $\Delta u(x)$, $\Delta d(x)$, etc. For gluons we will use the notation $V(x)$ and $\Delta V(x)$. In addition to data, we can use the Bjorken sum rule[15] in the form

$$\int_0^1 dx[\Delta u(x)-\Delta d(x)+\Delta\bar{u}(x)-\Delta\bar{d}(x)]=G_A/G_V\,, \tag{4.3}$$

where G_A/G_V is the ratio of the axial-vector to the vector coupling in neutron β decay. This ratio has the experimental value[16]

$$G_A/G_V=1.23\pm0.02\,.$$

It is apparent how Eq. (4.3) can be combined with measurements of $g_1^N(x)$ for some range of x to extrapolate over x between 0 and 1. We have another important constraint on the distribution functions using the projection of the z component of angular momentum. This gives

$$\begin{aligned}\langle J_z\rangle=\tfrac{1}{2}=\tfrac{1}{2}\int_0^1 dx[\Delta u(x)+\Delta d(x)+\Delta s(x)]\\ +\int_0^1 dx[\Delta V(x)]\\ +\frac{1}{2}\int_0^1 dx[\Delta\bar{u}(x)+\Delta\bar{d}(x)+\Delta\bar{s}(x)]\\ +\langle L_z\rangle\,,\end{aligned} \tag{4.4}$$

where $\langle L_z\rangle$ is the expectation value of the z component of orbital angular momentum summed over all the constituents. Equation (4.4) involves the gluon distribution ΔV as well as those of the quarks. When dealing with lepton processes, various authors[17,18] have lumped the contribution of gluons to Eq. (4.4) together with the $\langle L_z\rangle$ term. For our purposes, however, it is important to make the distinction above since spinning gluons are available for hard scattering. Estimates of $\langle L_z\rangle$ involve detailed models for the proton wave function and for the effective spin-orbit potential.

We will now consider three separate models for the spinning quark and gluon distribution functions. These will serve as illustrations, indicative of the range of possibilities allowed by present experimental measurements of the deep-inelastic lepton-proton spin-spin asymmetry.

Conservative SU(6) distributions

The starting point for most of our ideas on the spin content of the proton is SU(6). In this picture all the spin of the proton is carried by its valence quarks and we have approximately

$$\begin{aligned}\int_0^1 dx\,\Delta u(x)=\tfrac{4}{3}\quad[\text{SU(6) limit}]\,,\\ \int_0^1 dx\,\Delta d(x)=-\tfrac{1}{3}\quad[\text{SU(6) limit}]\,.\end{aligned} \tag{4.5}$$

We know that this cannot be exactly correct since we could insert Eq. (4.5) into the Bjorken sum rule Eq. (4.3) to obtain

$$G_A/G_V\,|_{\mathrm{SU(6)}}=\tfrac{5}{3}\,, \tag{4.6}$$

which disagrees with the experimentally measured value. It is an interesting exercise to think about how the result Eq. (4.5) can be modified without doing injustice to the spirit of a very successful (and simple) picture.

One possibility is to take seriously the idea that a proton has $L=0$ since this fact is involved in the proton's SU(6) spectroscopic classification. However, just as antiquarks and gluons are known to carry some of the momentum of the proton, it may also be necessary that they carry some of the spin. We can implement this speculation in a way which remains faithful to the SU(6) classification of a proton to obtain what we refer to as the conservative SU(6) distribution functions. For simplicity we will assume flavor-SU(3) invariance for the sea and denote

$$\bar{u}(x)=\bar{d}(x)=\bar{s}(x)=\bar{q}(x)\,. \tag{4.7}$$

We do not assume the sea antiquarks to be unpolarized but instead take a simple ansatz based on a study of perturbation-theory diagrams in QCD and the generation of the sea[8]:

$$\begin{aligned}\lim_{x\to1}\bar{q}_{++}(x)=c(1-x)^n[2+(1-x)^2]\,,\\ \lim_{x\to1}\bar{q}_{-+}(x)=c(1-x)^n[1+2(1-x)^2]\,.\end{aligned} \tag{4.8}$$

To see how much spin can reasonably be expected to reside in the sea (at values of Q^2 consistent with current experiments) we match the normalization of the antiquark distribution deduced from massive-lepton-pair data at $x=0.3$ (Ref. 19),

$$\bar{q}(x) \simeq \frac{0.6}{x}(1-x)^{10}. \tag{4.9}$$

We therefore postulate the simple parametrization

$$\begin{aligned} \bar{q}_{++}(x) &= \frac{0.13}{x}(1-x)^{10}[2+(1-x)^2], \\ \bar{q}_{-+}(x) &= \frac{0.13}{x}(1-x)^{10}[1+2(1-x)^2], \\ \Delta\bar{q}(x) &= 0.13(1-x)^{10}(2-x). \end{aligned} \tag{4.10}$$

The amount of spin which can be associated with the antiquarks and the "sea" component of quarks in this simple model is therefore

$$\begin{aligned} 2\langle s_z\rangle_{\bar{q}} &= 2\times 3\times \tfrac{1}{2}\int dx\,\Delta\bar{q}(x) \\ &= 0.068 \text{ [using (4.10)]}. \end{aligned} \tag{4.11}$$

It is possible, therefore, that antiquarks can contribute a small but non-negligible component to the spin of the proton. The idea that the antiquarks in the sea of a spinning proton might be polarized can be tested experimentally through the production of massive lepton pairs using polarized beam and target.[8] However, the contribution to the large-p_T production asymmetries we are discussing here from processes involving antiquarks will not be significant if $\bar{q}$ asymmetries are as small as given in Eq. (4.10).

The picture discussed here for antiquarks necessarily implies that the gluons in the proton are polarized. This is because antiquarks arise from the (virtual) pair creation from gluons and the gluons must be polarized to transmit spin information. Therefore, experiments which are sensitive to the polarization of antiquarks will also be able to indicate indirectly whether or not gluons carry spin information. Using an ansatz for gluon distribution functions based on ideas similar to that for antiquarks we can parametrize

$$\begin{aligned} V_{++}(x) &= \frac{c}{x}(1-x)^n[2+(1-x)^2], \\ V_{-+}(x) &= \frac{c}{x}(1-x)^n[1+2(1-x)^2]. \end{aligned} \tag{4.12}$$

The normalization of these distributions is now fixed by the momentum sum rule

$$\begin{aligned} \langle x\rangle_V &= \int_0^1 dx\, x\, V(x) \cong \tfrac{1}{2}, \\ c &= \frac{(n+1)(n+3)}{6(2n+4)}, \end{aligned} \tag{4.13}$$

and we can quickly estimate the contribution from the gluons to the z component of angular momentum

$$\langle s_z\rangle_V = \int_0^1 dx[\Delta V(x)] \cong \frac{1}{6}\left(\frac{2n+3}{2n+4}\right)\left(\frac{n+3}{n+2}\right), \tag{4.14}$$

$$\begin{aligned} \langle s_z\rangle_V &= 0.176 (n=6), \\ &\quad 0.174 (n=8). \end{aligned} \tag{4.15}$$

In fact, on the basis of the ansatz of Eq. (4.12) we can write

$$\langle s_z\rangle_V = \tfrac{1}{3}\langle x\rangle_V\left(1+O\left(\frac{1}{n}\right)\right), \tag{4.16}$$

where n is the effective power of $(1-x)$ appropriate for the gluon distribution. We expect it to be intermediate between the power of the valence-quark distribution and that of the sea-antiquark distribution. In our calculations we will use Eqs. (4.12) and (4.13) with $n=6$.

Using our models for antiquark and gluon distributions we can now isolate the contribution of the valence quarks to the spin of the proton. Because we are assuming $\langle L_z\rangle = 0$, we have from Eqs. (4.3), (4.10), (4.11), (4.12), and (4.14)

$$\tfrac{1}{2} \cong \tfrac{1}{2}\int_0^1 (\Delta u + \Delta d)\,dx + 0.068 + 0.176. \tag{4.17}$$

This can now be combined with the Bjorken sum rule in

$$\begin{aligned} 0.26 &\cong \tfrac{1}{2}\int_0^1 [\Delta u(x) + \Delta d(x)]\,dx, \\ 1.23 &\cong \int_0^1 [\Delta u(x) - \Delta d(x)]\,dx. \end{aligned}$$

The sea contribution to the Bjorken sum rule vanishes in our approximation due to isospin invariance. A similar value for the amount of spin carried by valence quarks was derived by Sehgal[20] by combining the Bjorken sum rule with the analog sum rule for the decay $\Xi^- \to \Xi^0 e^- \bar{\nu}_e$ and using SU(3) to obtain

$$\langle s_z\rangle_{\text{quarks}} = 0.30.$$

This is in reasonable agreement with

$$\langle s_z\rangle_{\text{quarks}} = 0.26$$

from our simple model.

We now consider the spinning quark distributions. For simplicity, we assume that

$$\begin{aligned} \Delta u(x) &\propto u^{\text{valence}}(x) = u(x) - \bar{u}(x), \\ \Delta d(x) &\propto d^{\text{valence}}(x) = d(x) - \bar{d}(x). \end{aligned}$$

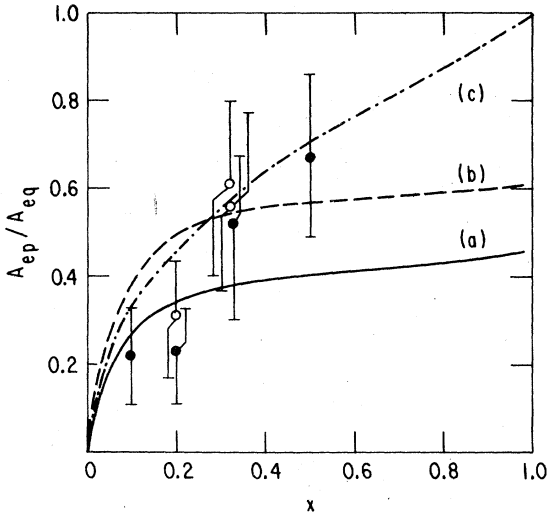

FIG. 7. Asymmetry ratio for polarized e-p scattering compared to predictions of various quark distributions: (a) conservative SU(6) model, (b) diquark model, (c) Carlitz-Kaur model. Solid circles are data from Ref. 14 and open circles are data from Ref. 13.

We can solve the constraints of Eq. (4.17) to obtain

$$\Delta u(x) \cong 0.44 u^{\text{valence}}(x),$$
$$\Delta d(x) \cong -0.35 d^{\text{valence}}(x).$$

For our model of the valence-quark distributions we take the parametrization of Field and Feynman.[21] The prediction for the deep-inelastic leptoproduction asymmetry using the conservative SU(6) distributions is displayed in Fig. 7. While these values are in rough agreement with experiment, there is a possible tendency to underestimate the data at large x. We will now turn to another approach to quark distributions.

Diquark distributions

Instead of relying on nonrelativistic SU(6) ideas, we can take a different approach. One picture, advocated by Field and Feynman,[21] assumes that, in certain limits, the proton can be treated as a quark-diquark system. This leads to the result that, for a large momentum proton, the fastest (or leading) quark has the same isospin and helicity as the proton itself. This idea has already received partial support from the experimental result[22]

$$\lim_{x\to 1} \frac{\nu W_2^{en}(x)}{\nu W_2^{ep}(x)} \approx \tfrac{1}{4},$$

but spin asymmetry measurements at large x have not tested this hypothesis.

In order to implement the quark-diquark picture and maintain consistency with the Bjorken and $\langle J_z \rangle$ sum rules, we have taken the distributions

$$\Delta u(x) = 0.61 u^{\text{val}}(x),$$
$$\Delta d(x) = \Delta s(x) = \Delta \bar{q}(x) = 0, \tag{4.18}$$
$$\Delta V(x) = 0.$$

We refer to these as our diquark distributions. The prediction for the ep spin-spin asymmetry in this model is also shown in Fig. 7.

Carlitz-Kaur distributions

The final set of distributions we will consider was developed by Carlitz and Kaur.[23] In this model, valence quarks lose their "memory" of the parent proton's spin orientation through interactions with the ocean. In particular, at small x, the valence quarks lose completely their memory of the spin orientation of the proton.

Let $\sin^2\theta$ represent the probability that a valence quark's spin will change in interactions with the ocean. Denote the density of the ocean relative to the valence quarks by $N(x)$ and let $H(x)$ be the probability of a spin-flip interaction between valence and ocean. Then

$$\sin^2\theta \equiv \tfrac{1}{2} H(x) N(x) / [H(x) N(x) + 1].$$

Carlitz and Kaur then assume that ocean quarks and antiquarks are unpolarized and that gluons have a $(1-x)^2$ falloff [their result is not very sensitive to the power of $(1-x)$] and arrive at the expression

$$H(x) N(x) = H_0 (1-x)^2 x^{-1/2}. \tag{4.19}$$

The value $H_0 = 0.052$ is set by the Bjorken sum rule, Eq. (4.3).

Integration over the quark and antiquark contributions to $\langle J_z \rangle$ indicates that 11.6% of the proton's helicity is due to gluons. We parametrize the gluons's spin as before [see Eqs. (4.12) and (4.13)], but renormalize the integrated gluon spin to be 11.6% of the total. Hence, the Carlitz and Kaur (plus gluon) spin distributions are given by

$$\Delta u(x) = \cos[2\theta(x)] [u^{\text{val}}(x) - \tfrac{2}{3} d^{\text{val}}(x)],$$
$$\Delta d(x) = -\tfrac{1}{3} \cos[2\theta(x)] d^{\text{val}}(x), \tag{4.20}$$
$$\Delta s(x) = \Delta \bar{q}(x) = 0,$$
$$\Delta V(x) = 0.116 \left[\frac{(n+1)(n+2)}{(2n+3)} \right] (2-x)(1-x)^n,$$

where

$$\cos[2\theta(x)] = [1 + H_0 x^{-1/2} (1-x)^2]^{-1}$$

is the spin dilution factor. In Fig. 7, we display the prediction of the Carlitz-Kaur distributions for the spin-spin asymmetry in ep scattering.

B. Scale violations in spin distributions and fragmentation functions

Proper use of QCD ideas within the framework of the hard-scattering model demands the use of quark and gluon distribution functions and fragmentation functions which exhibit scaling violations. In order to test the sensitivity of our predictions of spin-spin asymmetries to these scaling violations we must construct a set of distribution functions and fragmentation functions for a spinning proton consistent with the predictions of QCD. In this section we describe briefly a method due to Altarelli and Parisi.[11]

Altarelli and Parisi approach the problem of finding the Q^2 dependence of the distributions in parton-model language. They define functions $P_{A_{h_A}B_{h_B}}(x)$ which give the probability for finding a parton of type B and helicity h_B with fraction x of the parent momentum "inside" a parton of type A and helicity h_A. These probabilities are calculable in renormalization-group-improved QCD perturbation theory. The sums $P_{AB}=P_{A_+B_+}+P_{A_-B_+}$ are used to obtain the Q^2-dependent fragmentation functions, as well as nonspinning scale-violating distributions. We can also define differences, $\Delta P_{AB}=P_{A_+B_+}-P_{A_-B_+}$. Altarelli and Parisi show that the integro-differential equations describing the behavior of the spinning and nonspinning distributions evolve separately but in similar fashions. Let $\xi=\ln(Q^2/Q_0^2)$. Then for quark or antiquark (q^i) and gluon (V) nonspinning and spinning distributions we have

$$\frac{dq^i}{d\xi}(x,\xi)=\frac{\alpha(\xi)}{2\pi}\int_x^1\frac{dy}{y}\left[q^i(y,\xi)P_{qq}(x/y)+V(y,\xi)P_{qV}(x/y)\right],$$

$$\frac{dV}{d\xi}(x,\xi)=\frac{\alpha(\xi)}{2\pi}\int_x^1\frac{dy}{y}\left[\sum_{i=1}^{2f}q^i(y,\xi)P_{Vq}(x/y)+V(y,\xi)P_{VV}(x/y)\right] \tag{4.21a}$$

and

$$\frac{d\Delta q^i}{d\xi}(x,\xi)=\frac{\alpha(\xi)}{2\pi}\int_x^1\frac{dy}{y}\left[\Delta q^i(y,\xi)\Delta P_{qq}(x/y)+\Delta V(y,\xi)\Delta P_{qV}(x/y)\right],$$

$$\frac{d\Delta V}{d\xi}(x,\xi)=\frac{\alpha(\xi)}{2\pi}\int_x^1\frac{dy}{y}\left[\sum_{i=1}^{2f}\Delta q^i(y,\xi)\Delta P_{Vq}(x/y)+\Delta V(y,\xi)P_{VV}(x/y)\right], \tag{4.21b}$$

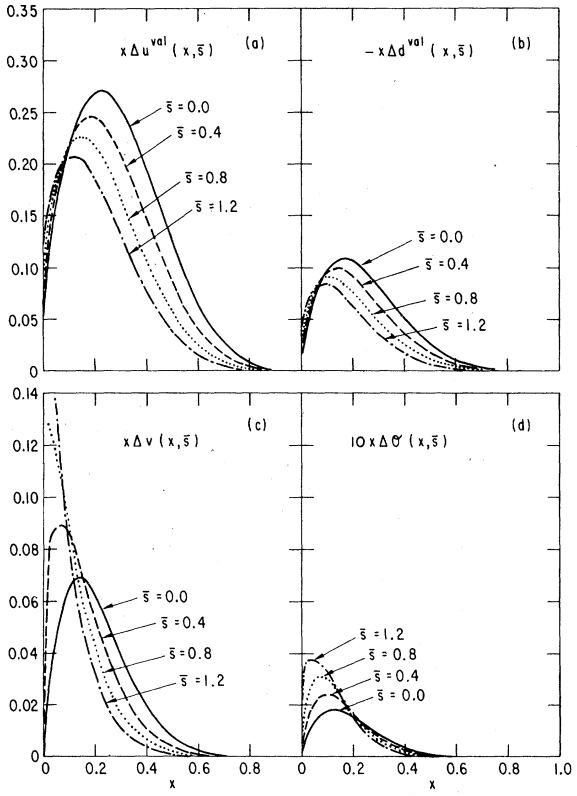

FIG. 8. Scale-violating conservative SU(6) spin distributions as functions of x and $\bar{s}=\ln[\ln(Q^2/\Lambda^2)/\ln(Q_0^2/\Lambda^2)]$: (a) valence u quarks, (b) valence d quarks, (c) gluons, (d) ocean antiquarks. Here $\Delta G(x,\bar{s})\equiv G_{++}(x,\bar{s})-G_{-+}(x,\bar{s})$.

where

$$\alpha(\xi)=\alpha(Q_0^2)\Big/\left[1+\left(\frac{33-2f}{12\pi}\right)\alpha(Q_0^2)\xi\right]$$

and f denotes the number of flavors. For the application of these scaling violations to large-p_T production we choose

$$Q^2=(\hat{s}\hat{t}\hat{u})^{1/3},$$

although other choices are possible.[1] The numerical methods we use for solving these equations are discussed in the Appendix. We have carried out the integration of the integro-differential equations (4.21) for the conservative SU(6) distributions with a starting value for Q^2 of $Q_0^2=2$ GeV^2. The results are shown in Fig. 8 as a function of longitudinal-momentum fraction x and

$$\bar{s}\equiv\ln\frac{\ln(Q^2/\Lambda^2)}{\ln(Q_0^2/\Lambda^2)}$$

with $\Lambda=0.5$ GeV. The behavior of the spinning distributions is very similar to that of the nonspinning distributions[24] (see Fig. 9), i.e., as Q^2 increases,

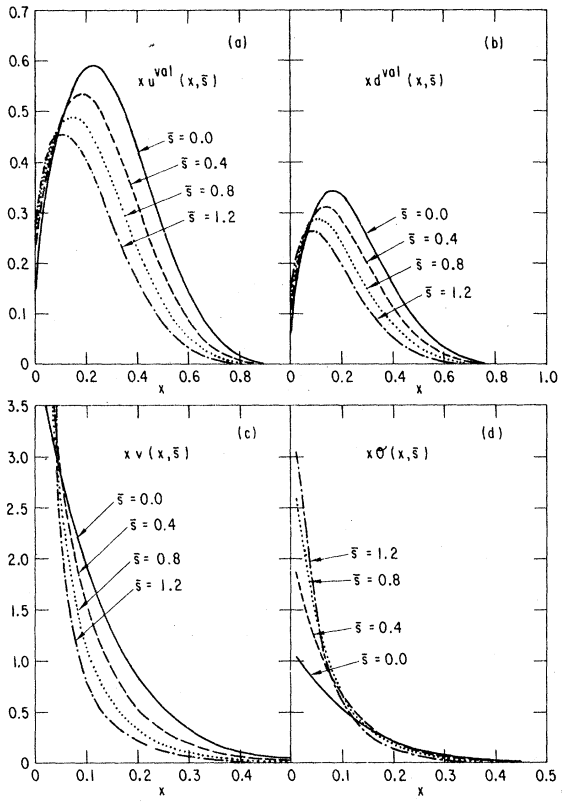

FIG. 9. Scale-violating nonspinning distributions as functions of x and $\bar{s}=\ln[\ln(Q^2/\Lambda^2)/\ln(Q_0^2/\Lambda^2)]$: (a) valence u quarks, (b) valence d quarks, (c) gluons, (d) ocean antiquarks.

more of the spin information and momentum of the valence quarks is fed into the low-x part of the ocean and gluon distributions.

It is instructive at this time to consider the effects of scaling violations on the Bjorken sum rule, Eq. (4.3), and on the $J_z=\frac{1}{2}$ sum rule, Eq. (4.4), which we have used to guide our considerations of spinning distributions. The simplest way to do this is to use the differential equations for the moments

$$\Delta m_n^i(\xi)=\int_0^1 \Delta q^i(x,\xi)x^{n-1}dx\,,$$

$$\Delta m_n^V(\xi)=\int_0^1 \Delta V(x,\xi)x^{n-1}dx\,,$$

which are

$$\frac{d}{d\xi}\Delta m_n^i(\xi)=\frac{\alpha(\xi)}{2\pi}\left[\Delta m_n^i \Delta A_n^{qq}+\Delta m_n^V(\xi)\Delta A_n^{qV}\right],$$

$$\frac{d}{d\xi}\Delta m_n^V(\xi)=\frac{\alpha(\xi)}{2\pi}\left[\sum_{i=1}^{2f}\Delta m_n^i(\xi)\Delta A_n^{Vq}+\Delta m_n^V(\xi)\Delta A_n^{VV}\right],$$

where the logarithmic exponents

$$\Delta A_n^{qq}=\int_0^1 \Delta P_{qq}(z)z^{n-1}dz\,,$$

etc., can be found in Ref. 11. For the sum rules Eqs. (4.3) and (4.4), we shall use the exponents

$$\Delta A_1^{qq}=0\,,\quad \Delta A_1^{qV}=0\,,$$

$$\Delta A_1^{Vq}=2\,,\quad \Delta A_1^{VV}=\frac{33-2f}{6}\,.$$

We can now differentiate the Bjorken sum rule with respect to ξ to obtain

$$\frac{d}{d\xi}(G_A/G_V)=\frac{\alpha(\xi)}{2\pi}\left[(\Delta m_1^u(\xi)+\Delta m_1^{\bar{u}}(\xi)-\Delta m_1^d(\xi)-\Delta m_1^{\bar{d}}(\xi)\Delta A_1^{qq}\right],$$

which vanishes since $\Delta A_1^{qq}=0$. The fact that the Bjorken sum rule is unaffected by scaling violations has been pointed out by Ahmed and Ross.[25] It is important in that our insight concerning the amount of spin carried by valence quarks obtained from this relation is not affected by scaling violations.

We can write the $J_z=\frac{1}{2}$ sum rule in the form

$$\tfrac{1}{2}=\langle s_z(\xi)\rangle_q+\langle s_z(\xi)\rangle_V+\langle L_z(\xi)\rangle\,,$$

where q includes a sum over quarks and antiquarks. With the approximations above, it is easy to see

$$\frac{d}{d\xi}\langle s_z(\xi)\rangle_q=0$$

since $\Delta A_1^{qq}=0$ and $\Delta A_1^{qV}=0$. This is related to the chiral invariance of the theory in our approximation of neglecting the masses of the quarks and the k_T dependence of the distribution functions. However, for gluons we have

$$\frac{d}{d\xi}\langle s_z(\xi)\rangle_V=\frac{\alpha(\xi)}{2\pi}\left[4\langle s_z(\xi)\rangle_q+\left(\frac{33-2f}{6}\right)\langle s_z(\xi)\rangle_V\right].$$

If the quantity in brackets on the right-hand side is positive the spin carried by gluons will increase without bound. Of course, with these assumptions we must have

$$\frac{d}{d\xi}\langle L_z(\xi)\rangle=-\frac{d}{d\xi}\langle s_z(\xi)\rangle_V\,.$$

With the assumptions we have discussed above for the distribution functions, $\langle s_z(\xi)\rangle_V$ will be positive and $\langle L_z(\xi)\rangle$ negative at large enough ξ. Our assumption that L_z vanished for the proton wave function cannot, therefore, be Q^2 independent

Owens[26] has shown that a simple alteration in the equations of Altarelli and Parisi suffices to allow for the calculation of scale-violating fragmentation functions, $D_c^h(z,Q^2)$. One again employs the notion

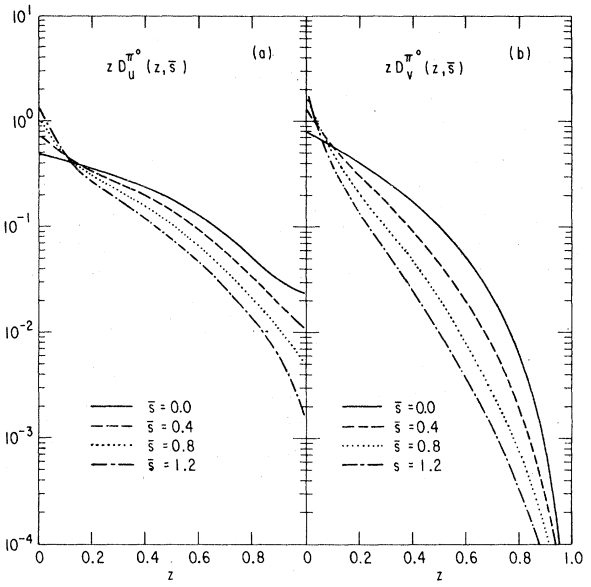

FIG. 10. Scale-violating fragmentation functions as functions of z and $\bar{s} = \ln[\ln(Q^2/\Lambda^2)/\ln(Q_0^2/\Lambda^2)]$: (a) u quark decaying into π^0, (b) gluon decaying into π^0.

of "partons inside partons" to obtain the equations

$$\frac{d}{d\xi} D_{q_i}^h(z,\xi) = \frac{\alpha(\xi)}{2\pi} \int_z^1 \frac{dy}{y} [D_{q_i}^h(y,\xi) P_{qq}(z/y) + D_V^h(y,\xi) P_{Vq}(z/y)] ,$$

$$\frac{d}{d\xi} D_V^h(z,\xi) = \frac{\alpha(\xi)}{2\pi} \int_z^1 \frac{dy}{y} \left[\sum_{i=1}^{2f} D_{q_i}^h(y,\xi) P_{qV}(z/y) + D_V^h(y,\xi) P_{VV}(z/y) \right] . \quad (4.22)$$

Our results for $D_u^{\pi^0}(z,Q^2) = D_{\bar{u}}^{\pi^0}(z,Q^2) = D_d^{\pi^0}(z,Q^2) = d_{\bar{d}}^{\pi^0}(z,Q^2)$ and $D_V^{\pi^0}(z,Q^2)$ using the starting fragmentation functions of Field and Feynman[21] and Eq. (2.34) of Ref. 2 are presented in Fig. 10 (see also Ref. 27). In general, the trend in $D_c^{\pi^0}(z,Q^2)$ is for more low-z π^0's to be produced and less high-z π^0's as Q^2 increases.

V. RESULTS OF OUR CALCULATION OF SPIN-SPIN ASYMMETRIES

In this section, we present some of the predictions of the QCD hard-scattering model for the spin asymmetry A_{LL}. When using scaling distributions, we will express our results as a function of $x_\perp = 2p_T/\sqrt{s}$. We will be more explicit about how the resuls might be expected to change as a function of p_T and $\sqrt{s}$ separately when discussing our calculations with scale-violating distribution functions. Unless otherwise specified, the center-of-mass scattering angle $\theta_{\text{c.m.}}$ is taken to be 90°.

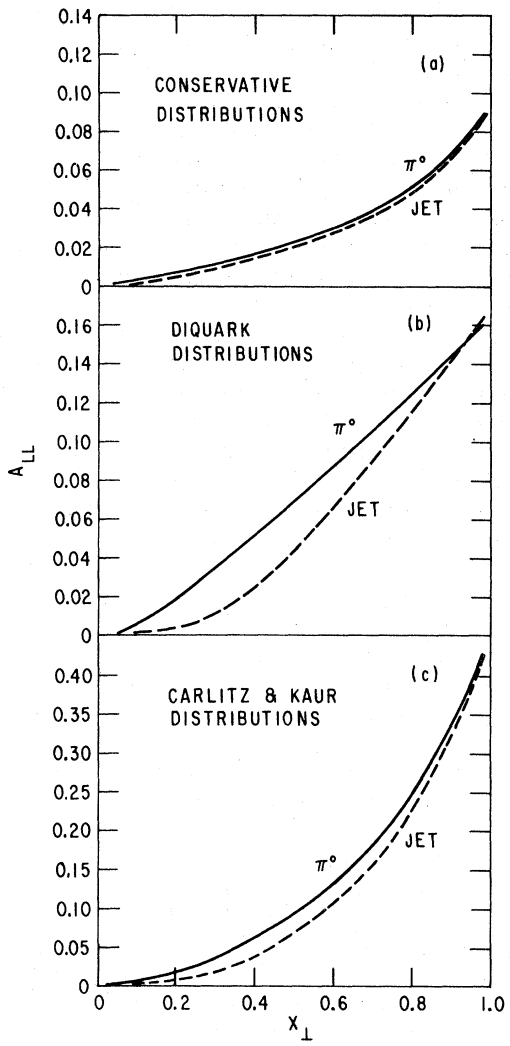

FIG. 11. Asymmetry A_{LL} for reactions $pp \to (\pi^0$ or jet$)+X$ as a function of $x_\perp = 2p_T/\sqrt{s}$ for (a) conservative SU(6) distributions, (b) diquark distributions, and (c) Carlitz-Kaur distributions.

Figure 11 presents the predictions for A_{LL} for proton-proton scattering and π^0 or jet production using the conservative SU(6), diquark, and Carlitz-Kaur models for the constituent distribution functions. For the conservative SU(6) and Carlitz-Kaur models, the gluon distribution parameter n [see Eq. (4.12)] has been set equal to 6. The dependence of A_{LL} on this parameter is such that the asymmetry increases slightly (a few percent) with decreasing n.

For both the π^0 and jet production reactions, the largest asymmetry is given by the Carlitz-Kaur distributions, which predicts A_{LL} of 10% at $x_\perp \approx 0.5$ and A_{LL} approaching 45% as $x_\perp$ approaches 1.0. The diquark distributions yield values for A_{LL} of about half or less than the Carlitz-Kaur model

and the conservative SU(6) distributions predict the smallest asymmetry, with a maximum of only about 9% at $x_\perp \sim 1.0$. In spite of a factor of 10^3 difference between the spin-averaged total cross sections for $pp \to \pi^0 X$ and $pp \to \text{jet} + X$, the predictions for A_{LL} for π^0 and jet production are very similar in magnitude and shape for each model of the constituent distributions considered.

It is interesting to see how the total asymmetry is divided up among constituent reactions $qq \to q$, $qq \to V$, $qV \to q$, $qV \to V$, $VV \to q$, and $VV \to V$, where q stands for either a quark or an antiquark and the constituent given on the right of the reaction is that which either decays into a pion or becomes a jet of hadrons. Of course, in the diquark model, only those reactions involving the leading quark alone contribute to the total asymmetry. The constituent reactions contribute to A_{LL} in a similar manner for both the conservative SU(6) and Carlitz-Kaur distributions. In both of these models, the major contributor to A_{LL} for large $x_\perp$ ($x_\perp \gtrsim 0.7$) is the $qq \to q$ reaction. However, at small and moderate values of $x_\perp$, the $qV \to q$ reaction is important and, also at small $x_\perp$, the $qV \to V$ and $VV \to V$ reactions become important. For jet production, we again find that the $qq \to q$ reaction is dominant at large $x_\perp$. At small $x_\perp$, however, more reactions make sizable contributions to A_{LL} than in the case of π^0 production. In particular, those reactions involving the production of a gluon jet, i.e., $qV \to V$, $VV \to V$, and $qq \to V$, are much larger contributors to the jet production reaction than in the $pp \to \pi^0 X$ case. This is due to the assumption we make that very little of the gluon momentum is given to any one particle in its decay.

In Fig. 12, we compare the predictions for A_{LL} vs $x_\perp$ as a function of $\theta_{\text{c.m.}}$ for $pp \to \pi^0 X$. As indicated in the figure, A_{LL} can vary by as much as a factor of 2, as it does for $x_\perp \approx 0.4$ if we compare the predictions for $\theta_{\text{c.m.}} = 30°$ and 90°. However, at $x_\perp \approx 0.4$, we also see that for $\theta_{\text{c.m.}} = 60°$ as compared to 90°, A_{LL} decreases by only about 2%.

The QCD hard-scattering model predictions for A_{LL} for proton-antiproton scattering for the conservative SU(6), diquark, and Carlitz-Kaur models of the constituent distributions are presented in Fig. 13. For the reaction $p\bar{p} \to \pi^0 X$, the curves of A_{LL} vs $x_\perp$ for all three models of the constituent distributions give results similar to their predictions for the $pp \to \pi^0 X$ case, although the predicted values of A_{LL} for large $x_\perp$ are much larger in the $p\bar{p}$ case. This is due to the different natures of the valence compositions of the proton and antiproton. As for the pp reactions, quark-quark scattering dominates the large-$x_\perp$ region, but for $p\bar{p}$ scattering, $q\bar{q} \to q\bar{q}$ scattering is dominant, whereas in pp scattering, it is the $qq \to qq$ reaction which is of

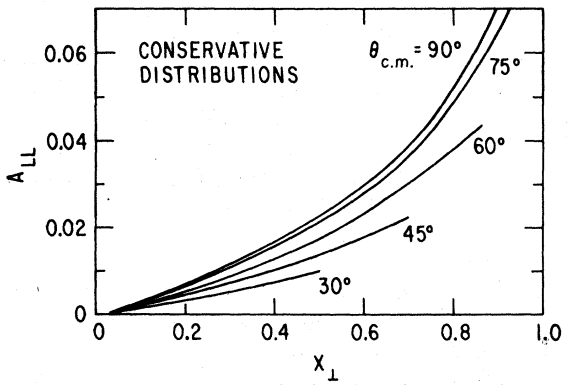

FIG. 12. Asymmetry A_{LL} for reaction $pp \to \pi^0 X$ as a function of $x_\perp = 2p_T/\sqrt{s}$ and $\theta_{\text{c.m.}}$.

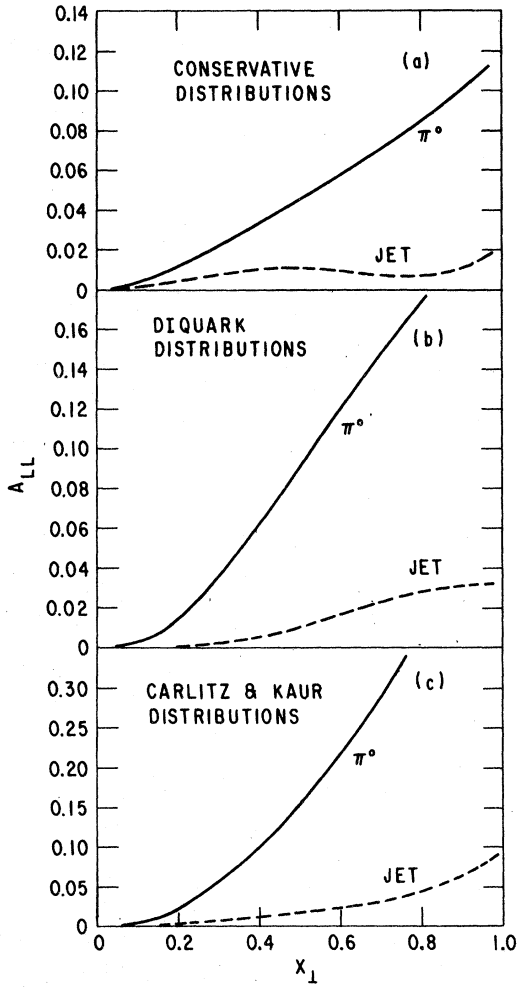

FIG. 13. Asymmetry A_{LL} for reactions $p\bar{p} \to (\pi \text{ or jet}) + X$ as a function of $x_\perp = 2p_T/\sqrt{s}$ for (a) conservative SU(6) distributions, (b) diquark distributions, and (c) Carlitz-Kaur distributions.

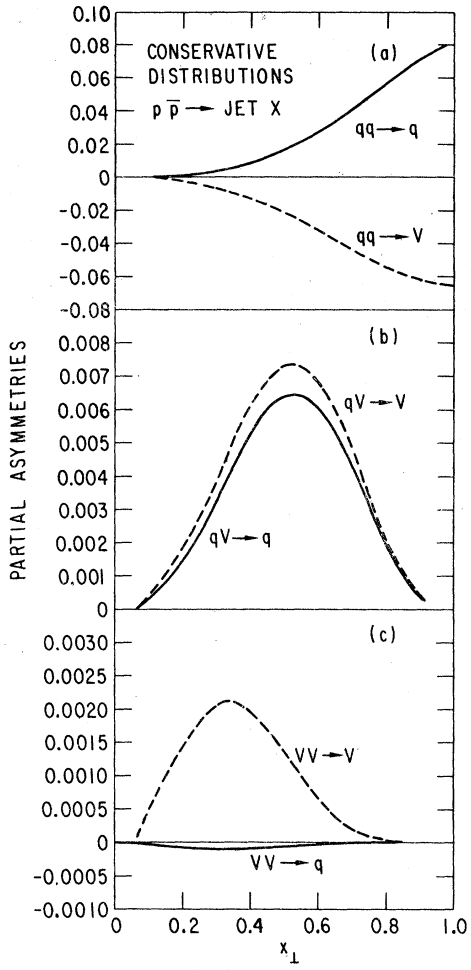

FIG. 14. Partial asymmetries for reaction $p\bar{p} \rightarrow$ jet $+X$ as functions of $x_\perp = 2p_T/\sqrt{s}$: (a) quark-quark, quark-antiquark, and antiquark-antiquark scattering, (b) quark-gluon and antiquark-gluon scattering, (c) gluon-gluon scattering.

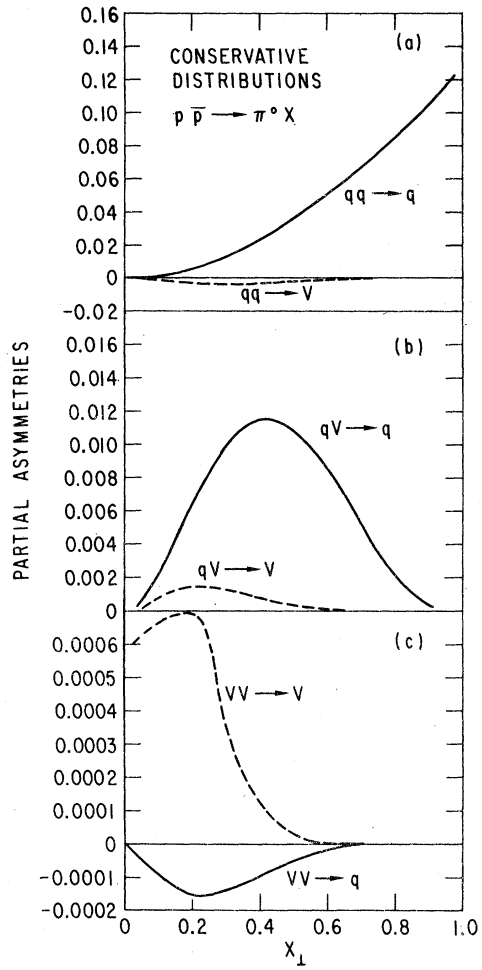

FIG. 15. Partial asymmetries for reaction $p\bar{p} \rightarrow \pi^0 X$ as functions of $x_\perp = 2p_T/\sqrt{s}$: (a) quark-quark, quark-antiquark, and antiquark-antiquark scattering, (b) quark-gluon and antiquark-gluon scattering, (c) gluon-gluon scattering.

importance.

The most striking aspect of the graphs of Fig. 13 is that, unlike the rather similar appearance of the π^0 and jet production graphs for proton-proton scattering, for the case of $p\bar{p}$ scattering, the π^0 and jet production curves for A_{LL} differ dramatically for all of the models of the constituent distributions we considered. In each case, the difference between π^0 and jet production for $p\bar{p}$ scattering is due to the increased importance in the jet cross sections of the $q\bar{q} \rightarrow V$ subprocess which competes now with the $qq \rightarrow q$ processes. The gluon fragmentation function $D_V^{\pi^0}$ [see Eq. (2.2)] serves to suppress this large, negative contribution to A_{LL} in the π^0-production case. (This effect can easily be seen in Figs. 14 and 15 in which the relative contributions of the constituent subprocesses for $p\bar{p}$ scattering are shown.)

A very sensitive test for the manner in which the proton's helicity is carried by its various constituents is given by a comparison of A_{LL} for π^+ vs π^- production in pp scattering, as can be seen in Fig. 16. Both the sign and magnitude (relative to π^+ production) of A_{LL} for π^- production are very dependent on the relationship between quark flavor and the ability to carry spin information in the proton. As we can see in Fig. 16, in the diquark model, for which all of the spin orientation information is carried by the leading u quark, $\Delta d(x) = 0$ and so for π^- production $A_{LL} \approx 0$. (A_{LL} is not exactly equal to zero but is, in fact, small and positive due to a contribution from the $uu \rightarrow uu$ subprocess. This is, however, suppressed by the smallness of $D_u^{\pi^-}$.) The sign of A_{LL} for π^- production is negative in

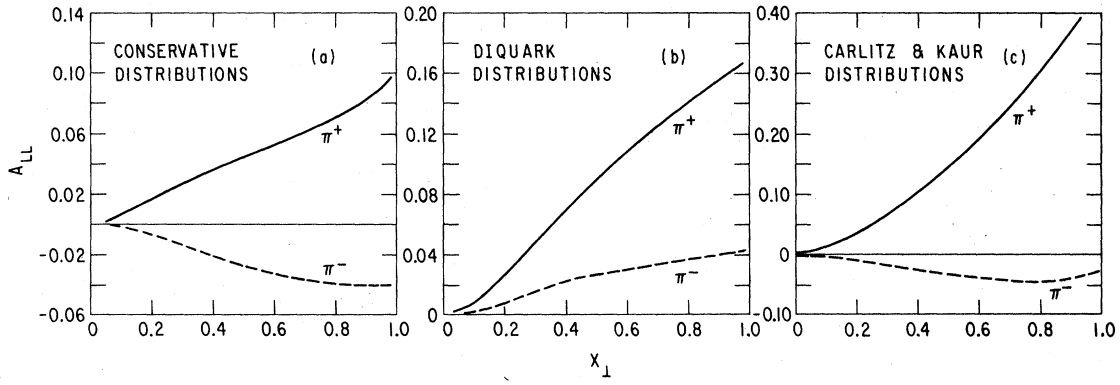

FIG. 16. Asymmetry A_{LL} for the reactions $pp \to \pi^{\pm} X$ as a function of $x_\perp = 2p_T/\sqrt{s}$ for (a) conservative SU(6) distributions, (b) diquark distributions, and (c) Carlitz-Kaur distributions.

both the conservative SU(6) and Carlitz-Kaur cases due to the negativity of $\Delta d(x)$ for these models. The relative magnitude of A_{LL} for π^- production to that for π^+ production reflects the degree to which spin information is carried by the d quark relative to the u quark in the spinning proton. For the conservative SU(6) model, $A_{LL}^{\pi^-}/A_{LL}^{\pi^+} \lesssim 0.4$ whereas for the Carlitz-Kaur model, $A_{LL}^{\pi^-}/A_{LL}^{\pi^+} \lesssim 0.1$, indicating that much less spin-remembering ability is attributed to the d quark in the Carlitz-Kaur model than in our SU(6)-like model.

The scale-violating spinning and nonspinning distributions displayed in Figs. 8 and 9 and the scale-violating fragmentation functions of Fig. 10 were also incorporated into our calculation of $pp \to \pi^0 X$. We found that A_{LL} still essentially scaled with $x_\perp$, retaining the same shape and increasing in magnitude by only about 5% at most for $\sqrt{s} = 80$ GeV as compared to $\sqrt{s} = 20$ GeV. This is due to the similarity of the coupled integrodifferential equations that describe the behavior of both the $G_{a(h_a)/A(\lambda_A)}$ and the $\Delta G_{a(h_a)/A(\lambda_A)}$ with x and Q^2; the effect just cancels out between numerator and denominator of A_{LL}. The fragmentation functions $D_c^{\pi^0}(z, Q^2)$ are, of course, the same for both numerator and denominator of A_{LL} and also tend to cancel. We expect that the k_T dependence of the spin and nonspin reactions should also cancel, again leaving A_{LL} essentially unchanged from our predictions.

At this point we would like to mention that calculations of spin-spin asymmetries have also been carried out recently by Cheng and Fishbach[28] both within the framework of perturbative QCD and in an "effective gluon" model. Since they use different parametrizations for the distribution functions, their QCD calculations do not agree in detail with ours but the overall pattern is similar.

VI. CONCLUSIONS

We have calculated the asymmetry A_{LL} for the inclusive production of pions and jets from proton-proton collisions or from proton-antiproton collisions. We have seen that this observable should provide a good test of the dynamical assumptions involved in the use of QCD perturbation theory in the hard-scattering model. The values of the asymmetries we find are sensitive to our assumptions for the spin-weighted quark and gluon distribution functions, but this ambiguity should diminish as better data on deep-inelastic electron-proton asymmetries become available.

We can make the following observations at this time. Comparison of asymmetries involving π^0's and jets should be a good test for the presence of large constituent-interchange model (CIM) contributions in $pp \to \pi^0 X$.[6] Because of trigger bias effects, CIM terms are much more important in $pp \to \pi X$ than in $pp \to \text{jet} + X$. Since the fundamental asymmetry for the CIM subprocess $\pi q \to \pi q$ must be zero, this could change our result that the $A_{LL}(pp \to \pi^0 X) \approx A_{LL}(pp \to \text{jet} + X)$. We also observe that the relationship between $A_{LL}(pp \to \pi^+ X)$ and $A_{LL}(pp \to \pi^- X)$ can provide interesting information concerning the correlations between spin and flavor in the proton wave function.

It would seem to be desirable that a program of large-p_T production experiments using polarized beam and target be carried out in the near future. An interesting set of measurements might be the following:

(1) A measurement of single-spin asymmetries which are assumed to vanish in the hard-scattering model.

(2) A study of the A dependence of large-p_T pro-

duction using polarized beams on nuclear targets.

(3) A measurement of spin-spin asymmetries such as the observable A_{LL} discussed here.

ACKNOWLEDGMENTS

Some of the calculations described here were done while Evelyn Monsay was a visitor at Brookhaven National Laboratory. She would like to thank the Brookhaven Theory Group for its hospitality. We have benefited during the course of this work from conversations with R. Field, T. Tudron, S. Wolfram, and A. Yokosawa. This work was performed under the auspices of the U. S. Department of Energy.

APPENDIX: NUMERICAL TREATMENT OF INTEGRODIFFERENTIAL EQUATIONS FOR SCALING VIOLATIONS

We would like now to turn our attention to the numerical treatment of Eqs. (4.21) and (4.22). We change variables from ξ to

$$\bar{s} = \ln \frac{\ln(Q^2/\Lambda^2)}{\ln(Q_0^2/\Lambda^2)} = \ln \frac{\alpha(Q_0^2)}{\alpha(Q^2)} .$$

We also assume a flavor-symmetric ocean and neglect charm,

$$u - u_{\rm val} = d - d_{\rm val} = \bar{u} = \bar{d} = s = \bar{s} = \Theta ,$$

$$\Delta u - \Delta u_{\rm val} = \Delta d - \Delta d_{\rm val} = \Delta\bar{u} = \Delta\bar{d} = \Delta s = \Delta\bar{s} = \Delta\Theta .$$

We feel that this is justified because spin-spin asymmetries of the type that we are calculating are not very sensitive to the presence of the ocean.

The functions $P_{qq}(x)$, $P_{qV}(x)$, $P_{Vq}(x)$, $P_{VV}(x)$ and their spin-dependent counterparts have been evaluated by Altarelli and Parisi.[11] Using their expressions and defining

$$z_p[f(x)] \equiv \ln(1-x)f(x) + \int_x^1 \frac{x}{y^2}\left[\frac{xf(y) - yf(x)}{y-x}\right] dy$$

we find for Eqs. (4.21a)

$$\frac{d}{d\bar{s}}[xq_i^{\rm val}(x,\bar{s})] = \frac{6}{27}\left\{2[xq_i^{\rm val}(x,\bar{s})] + \frac{4}{3}\int_x^1 \frac{x}{y^2}\left(1-\frac{x}{y}\right)[yq_i^{\rm val}(y,\bar{s})]dy + \tfrac{8}{3} z_p[xq_i^{\rm val}(x,\bar{s})]\right\},$$

$$\frac{d}{d\bar{s}}[x\Theta(x,\bar{s})] = \frac{6}{27}\left\{2[x\Theta(x,\bar{s})] + \tfrac{8}{3} z_p[x\Theta(x,\bar{s})] + \frac{4}{3}\int_x^1 \frac{x}{y^2}\left(1-\frac{x}{y}\right)[y\Theta(y,\bar{s})]dy + \frac{1}{2}\int_x^1 \frac{x}{y^2}\left[1 - \frac{2x}{y}\left(1-\frac{x}{y}\right)\right][yV(y,\bar{s})]dy\right\}, \quad \text{(A1)}$$

$$\frac{d}{d\bar{s}}[xV(x,\bar{s})] = \frac{6}{27}\left(\frac{33-2f}{6}\right)[xV(x,\bar{s})] + 6z_p[xV(x,\bar{s})] + 6\int_x^1 \frac{x}{y^2}\left(1-\frac{x}{y}\right)\left(\frac{x}{y}+\frac{y}{x}\right)[yV(y,\bar{s})]dy + \frac{4}{3}\int_x^1 \frac{1}{y}\left[1+\left(1-\frac{x}{y}\right)^2\right][yu^{\rm val}(y,\bar{s}) + yd^{\rm val}(y,\bar{s}) + 2fy\Theta(y,\bar{s})]dy\Bigg\},$$

where the equation for $xq_i^{\rm val}(x\bar{s})$ represents two equations: one for $xu^{\rm val}(x,\bar{s})$ and one for $xd^{\rm val}(x,\bar{s})$.

The set of equations (4.21b) becomes

$$\frac{d}{d\bar{s}}[x\Delta q_i^{\rm val}(x,\bar{s})] = \frac{6}{27}\left\{2[x\Delta q_i^{\rm val}(x,\bar{s})] + \tfrac{8}{3} z_p[x\Delta q_i^{\rm val}(x,\bar{s})] + \frac{4}{3}\int_x^1 \left(\frac{x}{y^2}\right)\left(1-\frac{x}{y}\right)[y\Delta q_i^{\rm val}(y,\bar{s})dy]\right\}$$

[identical to the equation for $xq_i^{\rm val}(x,\bar{s})$],

$$\frac{d}{d\bar{s}}[x\Delta\Theta(x,\bar{s})] = \left(\frac{6}{27}\right)\left\{2[x\Delta\Theta(x,\bar{s})] + \tfrac{8}{3} z_p[x\Delta\Theta(x,\bar{s})] + \left(\frac{4}{3}\right)\int_x^1 \left(\frac{x}{y^2}\right)\left(1-\frac{x}{y}\right)[y\Delta\Theta(y,\bar{s})]dy + \left(\frac{1}{2}\right)\int_x^1 \left(\frac{x}{y^2}\right)\left[2\left(\frac{x}{y}\right)-1\right][y\Delta V(y,\bar{s})]dy\right\}, \quad \text{(A2)}$$

$$\frac{d}{d\bar{s}}[x\Delta V(x,\bar{s})] = \left(\frac{6}{27}\right)\left(\left(\frac{4}{3}\right)\left\{\int_x^1 \frac{x}{y^2}\left(2-\frac{x}{y}\right)[y\Delta u^{\rm val}(y,\bar{s}) + y\Delta d^{\rm val}(y,\bar{s}) + 2fy\Delta\Theta(y,\bar{s})]\right\} + \left(\frac{33-2f}{6}\right)x\Delta V(x,\bar{s}) + 12\int_x^1 \frac{x}{y^2}\left(1-\frac{x}{y}\right)[y\Delta V(y,\bar{s})]dy + 6z_p[x\Delta V(x,\bar{s})]\right).$$

The overall scheme that was adopted for the numerical solution of these equations is as follows:

(1) Evaluate the structure functions at a set of "support points" $\{x_2\}$ which lie in the range (0, 1).

(2) From the values of the structure functions at the "support points" form an interpolating function which will give an analytic approximation to the function at all x in (0, 1). It is necessary to do this because the distribution functions will only be known at the "support points" which are the lower limits in the y integrals in Eqs. (A1) and (A2) after the first step in s, and the points selected for numerical integration will not, usually, coincide with the support points.

(3) Calculate the integrals and add them in a manner that is dictated by the $\bar{s}$-stepping algorithm (to be described later) at the support points. We are now back at the beginning and the whole procedure can be repeated.

It is necessary to realize, however, that the integro-differential equations will generate nonanalytic behavior at $x=0$ and $x=1$ in the form of $(\ln x)^k g(x)$ terms and $[\ln(1-x)]^j h(x)$ terms, respectively. To get around this problem we divided the range (0, 1) into four patches—A: (0.01, 0.1), B: (0.1, 0.5), C: (0.5, 0.9), and D: (0.9, 0.99). In patches A and B we changed variables to $z=\ln x$. That is, the interpolations and integrations were done in the variable z in patches A and B. In the patches A and B a function such as $(\ln x)^k g(x)$ becomes $z^k g(e^z)$ which is perfectly analytic except at $|z| \to \infty$. This implies that the interpolation and integration schemes that we use will not be destroyed by the presence of nearby singularities. In patches C and D we interpolated and integrated in the variable $w=\ln(1-x)$. We see again that the nonanalytic behavior at $x=1$ is banished to $w \to -\infty$.

We now describe the selection of support points and the interpolation procedure, which are closely related. Consider an arbitrary patch with range $[a, b]$ in the variable h (either z or w). We choose the support points according to the following formula[29]:

$$h_k = \left(\frac{a}{2}\right)\left[1-\cos\frac{(2k-1)\pi}{2n}\right] + \left(\frac{b}{2}\right)\left\{1+\cos\left[\frac{(2k-1)\pi}{2n}\right]\right\} .$$

The interpolating function $F(h)$ can be written as an expansion in Chebyshev polynomials:

$$F(h) = \sum_{j=0}^{n-1} C_j T_j^{[a,b]}(h) ,$$

where

$$T_j^{[a,b]}(h) = T_j\left(\frac{2h-b-a}{b-a}\right) ;$$

T_j is the usual Chebyshev polynomials defined on $(-1, 1)$ and

$$C_j = \frac{2}{n}\sum_{k=1}^{n} f(h_k)\cos\left[\frac{j\pi}{2n}(2k-1)\right] \quad (\text{for } j>0) ,$$

$$C_0 = \frac{1}{n}\left[\sum_{k=1}^{n} f(h_k)\right] .$$

This procedure is motivated by looking for a "mini-max" interpolating polynomial.[30] We chose $n=10$ (a total of 40 points with 4 patches). We factored out the dominant $(1-x)^n$ behavior before interpolating in patches C and D. The power n was always chosen to be that of the valence distributions. The answers were insensitive to a change in n of about 3 or 4. We found this interpolation procedure to have a fractional error of about 10^{-4} on (0.01, 0.99).

We used Gaussian quadrature to evaluate the integrals (recall that the integrands are highly analytic in z and w), with a support point in D getting N-point quadrature, and one in C getting $2N$-point quadrature. N was usually chosen to be 12, although the answers were not terribly sensitive to variations in N.

The algorithm for stepping the distributions in $\bar{s}$ was taken from Bulirsch and Stoer.[31] This algorithm uses a "modified midpoint rule" (a Runge-Kutta scheme whose error is given by a power series in the step size with only even powers) augmented by the use of Padé approximants of type II[32] to guess the continuous limit.

---

*Present address: Carnegie-Mellon University, Physics Department, Schenley Park, Pittsburgh, Pennsylvania 15213.

[1]R. D. Field, Phys. Rev. Lett. 40, 997 (1978); R. P. Feynman, R. D. Field, and G. C. Fox, Phys. Rev. D 18, 3320 (1978); J. F. Owens, E. Reya, and M. Glück, *ibid.* 18, 1503 (1978); A. P. Contogouris, R. Gaskell, and A. Nicolaidis, *ibid.* 17, 839 (1978); Prog. Theor. Phys. 58, 1238 (1977).

[2]R. Cutler and D. Sivers, Phys. Rev. D 17, 196 (1978).

[3]B. L. Combridge, J. Kripfganz, and J. Ranft, Phys. Lett. 70B, 234 (1977).

[4]In order to justify the use of Q^2-dependent distributions it is necessary to show that the infrared singularities

of QCD factorize in the manner suggested by the hard-scattering model. Significant progress on this topic has been made. See, for example, C. Sachrajda, Phys. Lett. 73B, 185 (1978) and *ibid.* 76B, 100 (1978); R. K. Ellis, H. Georgi, M. Machacek, H. D. Politzer, and G. C. Ross, Phys. Lett. 78B, 281 (1978); Y. L. Dokshitser, D. I. D'Yakonov, and S. I. Troyau, Proceedings of the XIII Winter School, Leningrad, 1978 (unpublished); S. Libby and G. Sterman, Phys. Lett. 78B, 618 (1978); Phys. Rev. D 18, 3252 (1978).

[5]J. Babcock, E. Monsay, and D. Sivers, Phys. Rev. Lett. 40, 1161 (1978).

[6]D. Sivers, S. J. Brodsky, and R. Blankenbecler, Phys. Rep. 23C, 1 (1976).

[7]For a simple discussion concerning the connection between *ep* asymmetry measurements and large-p_T inclusive asymmetries, see R. D. Field, in *Proceedings of the Symposium on Experiments using Enriched Antiproton, Polarized-Proton, and Polarized-Antiproton Beams at Fermilab Energies*, 1977, edited by A. Yokosawa (ANL, Argonne, Illinois, 1977).

[8]F. Close and D. Sivers, Phys. Rev. Lett. 39, 1116 (1977).

[9]I. P. Auer *et al.*, Fermilab Proposal No. 582 (unpublished).

[10]L. Kluberg *et al.*, Phys. Rev. Lett. 38, 670 (1977); U. Becker *et al.*, *ibid.* 37, 1731 (1976); R. McCarthy *et al.*, *ibid.* 40, 213 (1978).

[11]G. Altarelli and G. Parisi, Nucl. Phys. B126, 298 (1977).

[12]R. P. Feynman, *Photon-Hadron Interactions* (Banjamin, Reading, Mass., 1972).

[13]M. J. Algard *et al.*, Phys. Rev. Lett. 37, 1258 (1976); 37, 1261 (1976).

[14]M. J. Algard *et al.*, Phys. Rev. Lett. 41, 70 (1976).

[15]J. D. Bjorken, Phys. Rev. 148, 1467 (1966).

[16]Particle Data Group, Rev. Mod. Phys. 48, S1 (1976).

[17]F. E. Close, Nucl. Phys. B80, 269 (1974) and references therein.

[18]G. W. Look and E. Fischbach, Phys. Rev. D 16, 211 (1977).

[19]D. M. Kaplan *et al.*, Phys. Rev. Lett. 40, 435 (1978).

[20]L. M. Sehgal, Phys. Rev. D 10, 1663 (1974).

[21]R. D. Field and R. P. Feynman, Phys. Rev. D 15, 2590 (1977).

[22]H. L. Anderson *et al.*, Phys. Rev. Lett. 37, 4 (1976).

[23]R. Carlitz and J. Kaur, Phys. Rev. Lett. 38, 673 (1977); 38, 1102 (E) (1977); J. Kaur, Nucl. Phys. B128, 219 (1977).

[24]J. Kogut and J. Shigemitsu, Nucl. Phys. B129, 461 (1977); G. C. Fox, *ibid.* B131, 107 (1977).

[25]M. A. Ahmed and G. G. Ross, Phys. Lett. 56B, 385 (1975); Nucl. Phys. B111, 441 (1976).

[26]J. F. Owens, Phys. Lett. 76B, 85 (1978).

[27]G. C. Fox, invited talk presented at Orbis Scientiae, 1978, Coral Gables (unpublished).

[28]H.-Y. Cheng and E. Fischbach, Purdue University report, 1978 (unpublished).

[29]Z. Kopal, *Numerical Analysis*, 2nd edition (Wiley, N.Y., 1961).

[30]F. S. Acton, *Numerical Methods that Work* (Harper and Row, New York, 1970).

[31]R. Bulirsch and J. Stoer, Numerische Mathematik 8, 1 (1966).

[32]George Baker, Jr., *Essentials of Padé Approximants* (Academic, N.Y., 1975).